

On Markov chain Monte Carlo for sparse and filamentary distributions

Florian Maire Pierre Vandekerkhove

Abstract

A novel strategy that combines a given collection of π -reversible Markov kernels is proposed. It consists in a Markov chain that moves, at each iteration, according to one of the available Markov kernels selected via a state-dependent probability distribution which is thus dubbed *locally informed*. In contrast to random-scan approaches that assume a constant selection probability distribution, the state-dependent distribution is typically specified so as to privilege moving according to a kernel which is relevant for the local topology of the target distribution.

The second contribution is to characterize situations where a locally informed strategy should be preferred to its random-scan counterpart. We find that for a specific class of target distribution, referred to as *sparse and filamentary*, that exhibits a strong correlation between some variables and/or which concentrates its probability mass on some low dimensional linear subspaces or on thinned curved manifolds, a locally informed strategy converges substantially faster and yields smaller asymptotic variances than an equivalent random-scan algorithm.

The research is at this stage essentially speculative: this paper combines a series of observations on this topic, both theoretical and empirical, that could serve as a groundwork for further investigations.

F. Maire (Corresponding author),
SCHOOL OF MATHEMATICS AND STATISTICS
INSIGHT CENTRE OF DATA ANALYTICS
UNIVERSITY COLLEGE UNIVERSITY
BELFIELD, DUBLIN 4, IRELAND
E-mail address: `florian.maire@ucd.ie`

P. Vandekerkhove,
LABORATOIRE D'ANALYSE ET DE MATHÉMATIQUES APPLIQUÉES (UMR 8050)
UNIVERSITÉ PARIS-EST
F-77454 MARNE-LA-VALLÉE, FRANCE
E-mail address: `pierre.vandekerkhove@upem.fr`

1 Introduction

In this paper, we explore the problem of sampling from a specific family of probability distributions, generically denoted π , qualified as sparse and filamentary. This is typically the distribution of a random variable X defined on some measurable space $(\mathsf{X}, \mathcal{X})$ where X is a topological space, for example $\mathsf{X} \subseteq \mathbb{R}^d$ (for some $d > 0$) and \mathcal{X} is a sigma-algebra on X , such that X writes as

$$X := Z + \zeta. \tag{1}$$

In Eq. (1), Z is a random variable that takes its values on a compact subset $Z \subset X$ and ζ is an additive random perturbation. For instance, Z can be a uniform random variable on Z and ζ a Gaussian random variable with distribution $\mathcal{N}(0, \sigma^2)$. In this paper, we focus on situations where:

- The subset Z is a connected subspace of lower dimension compared to the ambient space X comprising for instance linear subspaces, hyperplanes, curved submanifolds, etc. In other words, for any point $z \in Z$ and a neighbourhood of z , say $\mathfrak{N}(z) \subset X$, the dimension of $\mathfrak{N}(z) \cap Z$ is (potentially significantly) lower than d . This feature characterizes the sparse structure of π , since the sampling problem is defined on a d -dimensional space while, locally and at the limit $\zeta \downarrow 0$, it can be reparameterized as a d' -dimensional space or submanifold with $d' < d$ (potentially $d' \ll d$).
- The probability mass of π is concentrated around Z . By analogy to electromagnetism, π has a filamentary structure where the probability mass in Z is regarded as the signal, say light, that glows in $X \setminus Z$ resulting in a halo effect. The signal-to-noise ratio is assumed to be reasonably high, *i.e.* our analysis focuses on the regime $\zeta \rightarrow 0$, almost surely.

Sparse and filamentary distributions arise in a number of statistical applications including Bayesian inverse problems (Knapik et al., 2011), models involving variables with strong nonlinear relationships (Givens and Raftery, 1996) and deterministic simulation models used in Ecology (Duan et al., 1992; Bates et al., 2003) and Demography (Raftery and Bao, 2010; Raftery et al., 1995), see also Poole and Raftery (2000) and the references therein for more applications. We also mention cosmic matter models in Cosmology, where the terminology *filamentary distribution* is also used (van de Weygaert et al., 2009; Tempel and Bussov, 2014).

Sampling from sparse and filamentary distributions usually represents a bottleneck when inferring models they arise in. In particular, simple Markov chain Monte Carlo methods (MCMC) such as the random-walk Metropolis-Hastings algorithm (RWMH) (Metropolis et al., 1953) or random-scan Gibbs sampler (RSGS) (see Geman and Geman (1984) and Liu et al. (1995) specifically for the random-scan approach) are known to be inefficient in this type of setup. Indeed, none of these two methods include information related to the local topology of the state space making them *de facto* unaware of ridge like features or locally unused or redundant dimensions.

Using *local information* to improve the mixing of the chain has generated an abundant research stream in the field statistical methodology, aiming at designing more sophisticated MCMC algorithms. The Markov chain generated by those methods typically moves according to position dependent information related to the target distribution: the gradient information (MALA) (Roberts and Stramer, 2002), the Hamiltonian dynamic (HMC) (Duane et al., 1987; Neal et al., 2011) or other information geometry objects (Girolami and Calderhead, 2011; Livingstone and Girolami, 2014). We also mention the regional adaptation approach proposed in Craiu et al. (2009) that leads to different optimal adaptive kernels in different region of the state space (see Andrieu and Thoms (2008) for an introduction on adaptive MCMC methods) and Conrad et al. (2016) that couple RWMH with a local quadratic approximation of the distribution of interest. These works have brought inspiring concepts and, to some extent, useful tools and softwares to practitioners (see for instance Carpenter et al. (2017)).

However, experienced users know that most of those methods are particularly computationally involved since they require some analytic quantities (Gradient, Hamiltonian integrator, Fisher Information matrix, etc.) to be calculated, routinely. More importantly, those methods are not specifically tailored to address the special case of sparse and filamentary distributions that features manifolds of lower dimension than

the ambient space (this is not the case of the aforementioned works) but are rather designed to sample from multimodal and/or heavy-tailed challenging distributions. Borrowing from geometric measure theory, [Diaconis et al. \(2013\)](#) develop a number of Monte Carlo algorithms to sample on manifolds. Although elegant, those methods remain challenging to generalize to practical problems. In practice, the most popular Bayesian approach to infer a posterior distribution where the signal is contained in a low-dimensional subspace drown into a background noise is to use an equivalent representation of the state space based on partitions as is the case in image segmentation applications. MCMC methods (and in particular variants of MH) have been successfully designed but the distribution of interest is defined on the space of possible configurations and not directly on \mathbf{X} . Nevertheless, we note that embedding a local information in the MH proposal such that an analysis of local level sets in ([Chang and Fisher, 2011](#)) or via the construction of local shape priors ([Erdil et al., 2016](#)), allows to speed up significantly the performance of algorithms. However, there is no clear theoretical investigation justifying the improvements observed with those methods. Perhaps, [Livingstone \(2015\)](#) and [Beskos et al. \(2018\)](#) represent the only relevant works that make precise theoretical statements on locally informed methods sampling from sparse and filamentary distributions, referred to therein as ridged densities. In [Beskos et al. \(2018\)](#), the authors study the proposal optimal scaling in a RWMH algorithm that samples from a ridged densities, in the spirit of [Roberts et al. \(1997\)](#). Interestingly, they show that when $d - d' \gg 1$, the diffusion regime is specified by a SDE and for optimality (in asymptotic regime) the RW proposal should be scaled, if the jump size is allowed to be position dependent, so that the RWMH acceptance rate is locally (*i.e.* dimension wise) 0.234. This is in line with the intuition that the jump size should be smaller in directions orthogonal to that containing the signal. In [Livingstone \(2015\)](#) (see also [Mallik and Jones \(2017\)](#) for a similar algorithm and an adaptive version of it), the author studies the efficiency (in non-asymptotic regime) of RWMH using a position dependent covariance matrix (an approach which actually gathers a number of the aforementioned method under a generic framework). In particular, it is established that for sparse and filamentary distributions and under regulatory assumptions, the convergence of the position dependent RWMH occurs at a geometric rate, something which does not always hold for the standard RWMH.

The approach followed in this paper can be seen as orthogonal to those previously explored in the literature: instead of designing a sophisticated MCMC method that is provably optimal in some sense, we propose and study a non-adaptive MCMC algorithm whose simplicity resembles that of RWMH and RSGS. Motivated by the results of [Livingstone \(2015\)](#) and [Beskos et al. \(2018\)](#), we tackle the two following questions:

Question 1. *Given a fixed collection of n π -invariant Markov kernels,*

$$\mathfrak{P} := P_1, P_2, \dots, P_n$$

that operate on different subspaces of \mathbf{X} and with different scaling factors, is it possible to find a π -invariant Markov chain that recursively moves according to a kernel selected from \mathfrak{P} by mean of a position dependent probability distribution $\omega := \omega(x)$ ($x \in \mathbf{X}$)?

Question 2. *If such algorithms exist, what can be said about their efficiency, both in terms of mixing time and in asymptotic regime, in the context of sparse and filamentary distributions and especially in the limiting case $\zeta \rightarrow 0$ almost surely? In particular, is it always preferable to use a position dependent selection probability $\omega(x)$ ($x \in \mathbf{X}$) compared to a position independent selection probability, *i.e.* where $\nabla_x \omega(x) = 0$?*

Related to Question 1 but in the specific context of the RSGS, [Latuszynski et al. \(2013\)](#) consider a class of Markov chains in which the kernel selection distribution

ω evolves and depends on the past history of the process. The author investigates conditions under which the Markov chain generated by this so-called adaptive RSGS algorithm is ergodic. In particular, the amount of adaptation of ω needs to be controlled and should eventually decrease to zero. As a result, should the adaptation scheme construct an optimal selection probability ω , the diminishing adaptation constraint imposes a *global* optimality. In some situations however, a globally optimal ω might only lead to a marginal improvement compared to a uniform probability and we argue that a position dependent selection probability $\omega(x)$ ($x \in \mathbf{X}$), perhaps not optimal in any sense, might be more efficient. Such situations include distributions that have a high degree of symmetry at a macro level but are locally anisotropic.

Far from reporting an exhaustive series of results related to locally informed MCMC applied to sparse and filamentary distribution, we present some facts both theoretical and empirical, some of them expected and other perhaps counter-intuitive, through a number of examples and algorithms that open up further research perspectives. The main contributions of this paper can be summarized as follows:

- (i) Method and applications: we construct two (non-adaptive) Markov chains (Algorithms 1 and 2), referred generically to as *locally informed*, that answer Question 1 (see Sections 4 and 5) and are implemented to sample from a variety of synthetic sparse and filamentary distributions, defined on discrete and general state spaces (Examples 1–7, throughout the paper).
- (ii) Theoretical and empirical observations (mainly addressing Question 2):
 - When $\mathfrak{P} = (P_1, \dots, P_n)$ are absolutely continuous kernels (as is the case in the RSGS), the locally informed MCMC Algorithm 1 is asymptotically sub-optimal, see Section 4.
 - On a specific discrete example (Example 1) and for the special case $\zeta = 0$ almost surely, we prove that the locally informed MCMC (Algorithm 1) is $\mathcal{O}(d)$ faster to converge than the non locally informed algorithm (Section 3).
 - We study how the theoretical results related to Example 1 transpose to the regime $\zeta \downarrow 0$. Since analytical results are more challenging to establish in presence of noise, most of our observations, apart from Examples 3 and 4, are based on empirical results. We find that the idea of “continuity” with the case $\zeta = 0$ is debatable, at least at a theoretical level.
 - In terms of mixing time, our locally informed algorithm presents a consistent convergence pattern. Convergence on the subspace \mathbf{Z} is faster than when using a non locally informed algorithm that uses the same kernels \mathfrak{P} but, as soon as ζ is not almost surely null, the exploration of $\mathbf{X} \setminus \mathbf{Z}$ slows down the convergence of locally informed algorithm, gradually as $\pi(\mathbf{X} \setminus \mathbf{Z})$ increases. These observations motivates the following conjecture:

Conjecture 1. *Comparing locally informed and non-locally informed, as defined in the context of this paper, a type of “The Tortoise and The Hare” scenario¹ is conjectured: the locally informed Markov chain converges quicker to a good approximation of π than its non locally informed competitor and there exists a finite pivot time at which the approximation offered by the non locally informed algorithm is better than the locally informed Markov chain.*
 - Empirically, we find that when the sparse and filamentary features of π are accentuated, this conjectured pivot time is sufficiently large to safely recommend using the locally informed algorithms for practical experiments, hence giving some credit to the methods developed in this paper.

¹In reference to the famous Aesop Fable.

2 Notation

Let $\mathsf{X} \subseteq \mathbb{R}^d$ and \mathcal{X} any sigma-algebra on X . We denote by $\Delta_n \subset \mathbb{R}^n$ the n -simplex *i.e.*

$$\Delta_n := \left\{ (\omega_1, \dots, \omega_n) \in \mathbb{R}^n, \sum_{i=1}^n \omega_i = 1, \text{ and } \omega_i \geq 0 \text{ for all } i \right\}. \quad (2)$$

For vectors $x \in \mathsf{X}$, we denote by $x_{i:j} := (x_i, \dots, x_j)$ with the convention that $x_{i:j} = \{\emptyset\}$ if $j < i$. Let $x_{-i} := (x_{1:i-1}, x_{i+1:d})$ and similarly for sets $A \in \mathcal{X}$, we denote by $A_{-i} = A_1 \times \dots \times A_{i-1} \times A_{i+1} \times \dots \times A_d$. For any subset $A \subset (\mathbb{R})$ and two positive integers p and q , $\mathcal{M}_{p,q}(A)$ denotes the set of $p \times q$ matrices whose elements belong to A . Let $\mathfrak{M}_1(\mathsf{X})$ be the set of probability measures on $(\mathsf{X}, \mathcal{X})$ and for any function $f : \mathsf{X} \rightarrow \mathbb{R}$ and any measure $\mu \in \mathfrak{M}_1(\mathsf{X})$ we define $\mu f := \int f d\mu$. Let $\mathcal{L}^2(\pi)$ be the set of π -measurable functions on X such that $\pi f^2 < \infty$ and $\mathcal{L}_0^2(\pi) := \{f \in \mathcal{L}^2(\pi), \pi f = 0\}$. For any Markov operator K on $(\mathsf{X}, \mathcal{X})$ we have that for all $x \in \mathsf{X}$, $K(x, \cdot) \in \mathfrak{M}_1(\mathsf{X})$ and for all $A \in \mathcal{X}$, $x \mapsto K(x, A) \in [0, 1]$ is a π -measurable function. Moreover, for any $f \in \mathcal{L}^2(\pi)$ and $\mu \in \mathfrak{M}_1(\mathsf{X})$, we will denote by

- $Kf : \mathsf{X} \rightarrow \mathbb{R}$, the measurable function defined as

$$Kf(x) := \int K(x, dy) f(y),$$

- $\mu K : \mathcal{X} \rightarrow (0, 1)$, the measure in $\mathfrak{M}_1(\mathsf{X})$ defined as

$$\mu K(A) := \int_{\mathsf{X}} \mu(dx) K(x, A).$$

For two Markov kernels P_1 and P_2 , P_1 dominates P_2 in the off-diagonal ordering (or Peskun ordering) [Peskun \(1973\)](#); [Tierney \(1998\)](#) and we denote $P_1 \succeq_P P_2$, if for all $A \in \mathcal{X}$

$$P_1(x, A \setminus \{x\}) \geq P_2(x, A \setminus \{x\}) \quad (3)$$

for π -almost all $x \in \mathsf{X}$. The total variation distance between two probability measures $(\pi, \nu) \in \mathfrak{M}_1(\mathsf{X})^2$ is defined as $\|\pi - \nu\| := \sup_{A \in \mathcal{X}} |\pi(A) - \nu(A)|$ and when the two distributions are absolutely continuous with respect to a common dominating measure $\lambda \in \mathfrak{M}_1(\mathsf{X})$, we have $\|\pi - \nu\| = (1/2) \int_{\mathsf{X}} |\pi(x) - \nu(x)| \lambda(dx)$. Finally, we will use the convention that a random variable (r.v.) is written in capital letter and realizations in small letter. The notation $X \rightsquigarrow x$ refers to the process of simulating X and calling x the observed outcome. $X \sim \pi$ means that X is a π -distributed random variable. For a r.v. X defined on a probability space $(\mathsf{X}, \mathcal{X}, \mathbb{P})$, δ_{x_0} denotes the degenerate distribution at some value $x_0 \in \mathsf{X}$, *i.e.* $\mathbb{P}(X = x_0) = 1$.

3 Introductory Examples

We start with three illustrative examples in which the distribution of interest is defined on a discrete state space. [Example 1](#) is an archetypical case of a sparse and filamentary distribution and highly advocates using a locally informed strategy over a simple RSGS algorithm, in terms of mixing time. [Example 2](#) is a noised version of [Example 1](#), in the sense of [Eq. \(1\)](#). The advantage of the locally informed approach observed in the noise-free case deteriorates as the noise increases and $d' \rightarrow d$, *i.e.* when π loses its sparse and filamentary structure. Moving further away from the sparse and filamentary framework, [Example 3](#) (in which there is no topology) presents a scenario where the locally informed strategy fails remarkably. Not much is said on our locally informed algorithm at this stage: its presentation and some theoretical properties are explored in [Sections 4 and 5](#).

Example 1. Let π be the distribution defined on $\mathbf{X} = \{1, \dots, m\}^d$ where $d \geq 2$ and $m \geq 3$. \mathbf{X} is regarded as a d -dimensional discrete hypercube where each edge length is m . The probability distribution π is uniform on $Z \subset \mathbf{X}$, a filament that comprises the connected edges $\mathcal{E}_1, \mathcal{E}_2, \dots, \mathcal{E}_d$ defined as follows:

$$Z := \bigcup_{i=1}^d \mathcal{E}_i, \quad \mathcal{E}_i := \{x \in \mathbf{X} \mid x_{1:i-1} = m \text{ and } x_i \in (1, m) \text{ and } x_{i+1:d} = 1\}. \quad (4)$$

The distribution π is illustrated graphically at Figure 1 for $m = 10$ and $d = 3$.

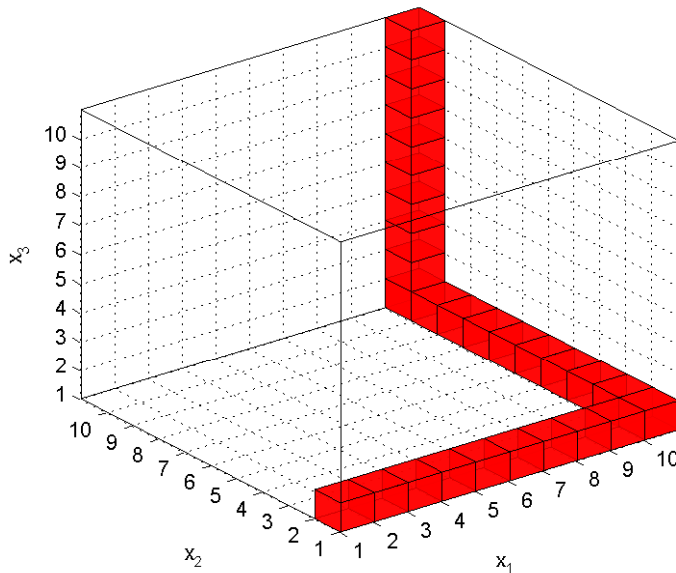


Figure 1: (Example 1 with $n = 10$ and $d = 3$) The filament Z are the states in red and all the mass of π is concentrated on Z .

Sampling from π is straightforward but for illustrative purpose we consider the two following MCMC algorithms:

- A random-scan Gibbs sampler (RSGS) that proceeds by picking a dimension $I \rightsquigarrow i$ uniformly at random, *i.e.* according to the distribution $I \sim \omega = \text{unif}\{1, \dots, d\}$ and then drawing the new state X' conditionally on the current state, say X , by refreshing only $X'_i \sim \pi(\cdot | X_{-i})$ and setting $X'_{-i} = X_{-i}$. Note that, with probability $1 - 1/d$, the selected dimension i will prevent to have $X' \neq X$ as $1 - 1/d$ full posterior distributions $\pi(\cdot | X_{-i})$ have their probability mass concentrated exclusively on X_i . Hence, when d is large, the Markov chain hardly moves.
- A locally informed sampler that proceeds by first picking a dimension $I \rightsquigarrow i$ with a non-uniform probability distribution $\omega(X) = (\omega_1(X), \dots, \omega_n(X))$ that depends on the current chain state $X \in \mathbf{X}$. More precisely, $\omega(X)$ is defined as follows: if X belongs to one and only one edge, say $X \in \mathcal{E}_i$, then $\omega(X) := \delta_i$ and if X belongs to two edges, say $X \in \mathcal{E}_i \cap \mathcal{E}_{i+1}$, then $\omega(X) := (1/2)\delta_i + (1/2)\delta_{i+1}$. Conditionally on X and i , a proposal X' is drawn as in the RSGS, *i.e.* $X' \sim \pi(\cdot | X_{-i})$, and is then

accepted as the next state of the Markov chain with probability $1 \wedge \omega_i(X')/\omega_i(X)$. If X' is rejected, the chain stays put at X . Intuitively, the distribution $\omega(X)$ is designed so that the sampler takes advantage of the topology by updating a component of X that moves the chain on the same edge but, contrarily to the RSGS, at a state different to X with high probability.

In what follows, for any quantity α defined in the RSGS, α^* will refer to the corresponding quantity for the locally informed algorithm. Propositions 1 and 2 suggest that, in this example, the locally informed strategy is $d/2$ times more efficient than the RSGS, where efficiency is measured as time to reach equilibrium. We recall the definition of a coupling time associated with a Markov kernel P .

Definition 1. Let $\{X_t, X'_t\}_t$ be a discrete time process defined on $(\mathsf{X} \times \mathsf{X}, \mathcal{X} \otimes \mathcal{X})$ such that marginally $\{X_t\}_t$ and $\{X'_t\}_t$ are both a Markov chain with transition kernel P with initial distribution μ and μ' , respectively. The coupling time of the joint process $\{X_t, X'_t\}_t$ is the random variable τ defined as:

$$\tau := \inf_{t \in \mathbb{N}} \{X_t = X'_t\}.$$

We recall that τ is a time characteristic to the Markov chain speed of convergence since the coupling inequality (see e.g. Lindvall (2002)) states that for all $t \in \mathbb{N}$,

$$\|\Pr\{X_t \in \cdot\} - \pi\| \leq \Pr\{\tau > t\}.$$

Proposition 1. In the context of Example 1, the expected coupling time of the RSGS is $d/2$ times larger than of the locally informed algorithm when both algorithms start at state $x_1 := (1, 1, \dots, 1)$, i.e.

$$\mathbb{E}_{x_1}(\tau) = \frac{d}{2} \mathbb{E}_{x_1}(\tau^*). \quad (5)$$

Proposition 2. Consider a delayed version of the locally informed Markov chain that moves according to P^* with probability $\lambda \in (0, 1)$ and remains to its current state with probability $1 - \lambda$. Then, in the context of Example 1, the RSGS and the locally informed Markov chain delayed by a factor $\lambda = 2/d$ converge to π at the same speed.

The proof of those two propositions can be found in Sections 8.1 and 8.2, respectively. They follow from a coupling argument applied to an equivalent representation of the Markov chains on a simpler state space.

Remark 1. The factor $d/2$ in the Propositions 1 and 2 can be interpreted as follows: since π is uniform on Z , the convergence of both Markov chains (starting from one extremity of the filament) is characterized by the speed at which they cross the hypercube vertices that belong to Z , e.g. $(10, 1, 1)$ and $(10, 10, 1)$ for the case illustrated in Figure 1. While at one of those vertices, the relative speed at which the RSGS moves to one of the two adjacent edges compared to the informed algorithm is $2/d$ since “only” two choices of direction may lead to such a transition. We have considered the slight change of definition of Z in the case $d = 3$ with $\mathsf{Z} := \mathcal{E}_1 \cup \mathcal{E}_2 \cup \mathcal{E}'_3$ where $\mathcal{E}'_3 := \{x \in \mathsf{X} \mid x_1 = m, x_2 = 1, x_3 \in (1, m)\}$. In this example, the state $(m, 1, 1)$ connects the three subspaces of dimension one. Hence, the RSGS and the informed algorithms are equally efficient to jump to any edge while at this state and we have verified theoretically that, in this case, the relative speed of convergence between the two algorithms is $d/3 = 1$.

To summarize, Example 1 confirms the intuition that a state dependent distribution $\omega(X)$ that incorporates geometric and topological information of π to draw the updating direction of a Gibbs sampler can speed up the Markov chain convergence. Again, we stress that obtaining those analytical results is eased by the fact that the mass of π is here concentrated on the filament, i.e. $p := \pi(\mathsf{X} \setminus \mathsf{Z}) = 0$. Nevertheless, this intuition can be generalized to the more realistic situation where the probability mass in the filament is immersed into an ambient noise. This is the purpose of Example 2.

Example 2. We consider the distribution π from Example 1, where now $p = \pi(X \setminus Z) > 0$.

We consider the two algorithms used in Example 1 to sample from π . The locally informed algorithm is implemented with a weight function extending that defined at Example 1. More precisely, if $X \in Z$, let the subset $\mathcal{S}(X) \subset \{1, \dots, d\}$ defined so that the update of any dimension $i \in \mathcal{S}(X)$ could take the next state of the Markov chain to $X \setminus Z$. The weight function ω used in the locally informed algorithm is defined as follows: if $X \in Z$, with probability p , pick the update direction uniformly at random on $\mathcal{S}(X)$ and with probability $1 - p$, pick the update direction uniformly at random on $\{1, \dots, d\} \setminus \mathcal{S}(X)$. When $X \notin Z$, the update direction is drawn uniformly at random on $\{1, \dots, d\}$. Figure 2 shows that the locally informed algorithm retains its advantage compared to RSGS even when $p > 0$, for moderate values of p . Interestingly, when p increases (e.g. $p = 0.1$) a shortcoming of the locally informed algorithm is exposed: it clearly outperforms RSGS in terms of exploring Z quickly but converges on $X \setminus Z$ extremely slowly. This is even more involved when the dimension d is small. Figure 3 illustrates theoretically this observation, when $d = 2$ and $p = 0.1$: in this case, the informed algorithm clearly trails behind the random scan algorithm. For example, the informed algorithm requires 25% more time than RSGS to reach a distribution which lies in a ball centered at π and radius 10^{-5} . Example 3 conceptualises this situation in a simplified setting and shows that when moving away from sparse and filamentary distributions, one should clearly avoid using the locally informed algorithm.

The following example showcases a scenario where π is not sparse and filamentary. In this case, π does not even have a topological structure and the convergence of a locally informed algorithm is shown to be much slower than a non locally informed algorithm using the same proposal kernels.

Example 3. We consider the distribution π defined on $X := \{1, 2, 3\}$ such that $\pi(1) = \pi(2)$ and $\pi(3) = p$, for some $p > 0$.

In order to sample from π , we consider Markov chains that attempt moves according to the following proposal distributions

$$Q_1(i, \cdot) = \delta_{\inf\{X \setminus \{i\}\}} \quad \text{and} \quad Q_2(i, \cdot) = \delta_{\sup\{X \setminus \{i\}\}}. \quad (6)$$

Put simply, Eq. (6) means that Q_1 and Q_2 attempt to visit a state which is not the current one. We consider an algorithm, that we refer to as uninformed, that picks the proposal independently from the current state of the Markov chain, i.e. with probability $\omega(i) = (1/2, 1/2)$. We compare this uninformed strategy with a locally informed proposal selection, that depends on the current state of the Markov chain. More precisely, if the Markov chain is at state i , it will attempt a move to a state $j \in X \setminus \{i\}$ with probability proportional to $\pi(j)$. This writes formally as $\omega(i) \propto (\pi(\inf\{X \setminus \{i\}\}), \pi(\sup\{X \setminus \{i\}\}))$. In other words, while the uninformed Markov chain attempts moving to states regardless their probability mass, the locally informed algorithm is more likely to attempt moving to states with larger probability mass. For both algorithms, the attempted moves are then accepted/rejected according to a probability that guarantees both Markov chains to be π -invariant:

- The usual Metropolis-Hastings acceptance ratio for the uninformed Markov chain.
- A slightly modification of the Metropolis-Hastings acceptance ratio for the locally informed Markov chain, see Algorithm 2 at Section 5.

We compare the two Markov chains according to their spectral properties. First, recall that for a reversible Markov chain with transition kernel P and spectrum $\text{Sp}(P)$, the spectral gap, defined as $\gamma(P) := 1 - \sup\{|\lambda|, \lambda \in \text{Sp}(P) \setminus \{1\}\}$, is used as a marker of speed of convergence, the larger the gap the faster the convergence, see e.g. Rosenthal (2003).

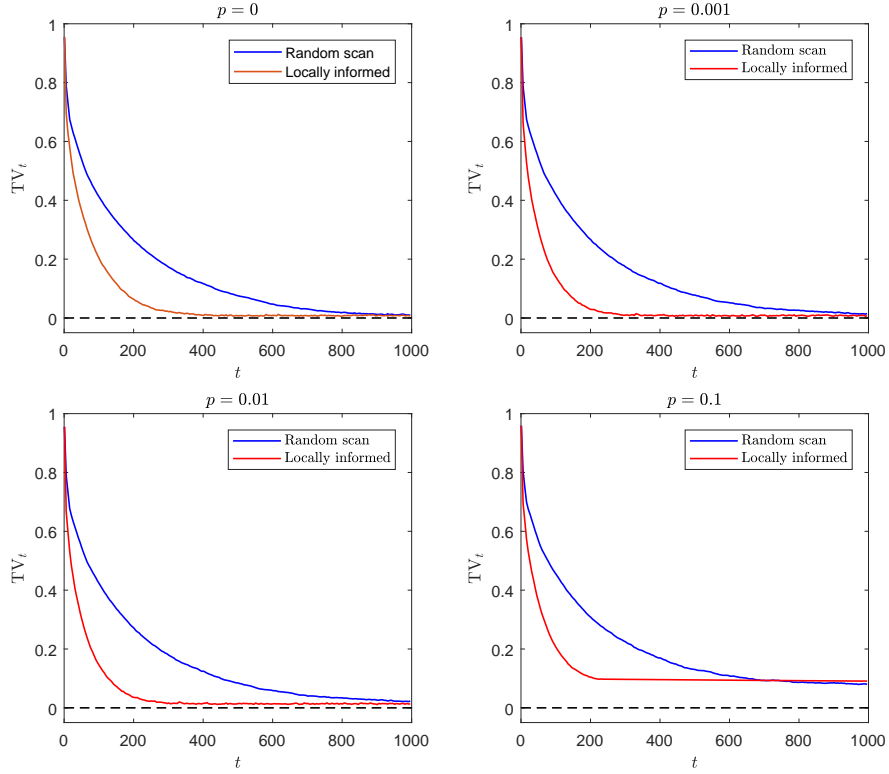


Figure 2: Examples 1 and 2 (Hypercube) in dimension $d = 7$ with $n = 4$ possible states per dimension and $p = \pi(\mathcal{X} \setminus \mathcal{Z}) \in \{0, 10^{-3}, 10^{-2}, 10^{-1}\}$. Convergence results (in total variation distance) are obtained from 50000 independent Markov chains simulated from the two possible algorithms, all starting from the state $(1, 1, \dots, 1)$. Note that those results could have been obtained theoretically but would have required handling routine operations on square matrices of dimension 16384, causing obvious computational difficulties.

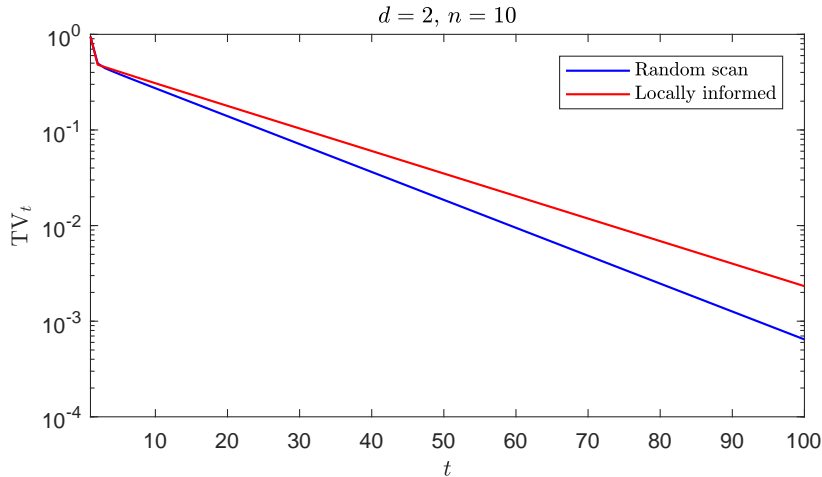


Figure 3: Example 2 (Hypercube) in dimension $d = 2$ with $n = 10$ possible states per dimension and $\pi(\mathcal{X} \setminus \mathcal{S}) = 10^{-1}$. Initial distribution is a dirac at one extremity of the two-dimensional filament. The total variation distances were calculated analytically.

Proposition 3. *In the context of Example 3 with $p \in (0, 1/3)$, let $\gamma(p)$ (resp. $\gamma^*(p)$) be the spectral gap of the Markov chain with uninformed proposal (resp. with locally informed proposal). Then, we have*

$$\gamma(p) = \frac{1-2p}{1-p} \quad \text{and} \quad \gamma^*(p) = p \frac{3-5p}{1-p^2},$$

and especially when $\epsilon \searrow 0$, $\gamma(p) = o(1)$ while $\gamma^*(p) = o(p)$.

The proof is postponed to Section 8.3. Proposition 3 states that it is more efficient in this scenario to propose highly frequent (risky) moves to state $\{3\}$ that are most of the time rejected (the uninformed chain) than essentially jumping between states $\{1\}$ and $\{2\}$ repeatedly (the locally informed chain). Hence perhaps counterintuitively, the uninformed chain that features $\mathbb{P}\{X_n = X_{n+1}\} \approx 1/2$ converges faster than the locally informed that features $\mathbb{P}\{X_n = X_{n+1}\} \approx 0$. In other words, the highly correlated chain is better than the risk averse one for this example, in the sense of convergence speed.

4 Locally informed algorithm for general Markov kernels

We consider a collection of n π -invariant Markov kernels

$$\mathfrak{P} := P_1, P_2, \dots, P_n,$$

i.e. for any $i \in \{1, \dots, n\}$ and $A \in \mathcal{X}$, $\pi P_i(A) := \int_{\mathcal{X}} \pi(dx) P_i(x, A) = \pi(A)$. If, in addition, each kernel is irreducible and aperiodic, then any Markov chain that makes use (perhaps randomly) of one of those kernels to transition from one state to another will converge to π . One can readily check that in the case of a random selection $\omega \in \Delta_n$ (where Δ_n is the n -simplex defined at (2)), the Markov kernel writes $P_\omega := \sum_{i=1}^n \omega_i P_i$

and satisfies for any $A \in \mathcal{X}$

$$\begin{aligned} \pi P_\omega(A) &= \int \pi(dx) P_\omega(x, A) = \int \pi(dx) \sum_{i=1}^n \omega_i P_i(x, A) \\ &= \sum_{i=1}^n \omega_i \int \pi P_i(x, A) = \sum_{i=1}^n \omega_i \pi(A) = \pi(A). \end{aligned} \quad (7)$$

In [Roberts and Rosenthal \(1997\)](#) and [Roberts and Rosenthal \(1998b\)](#), the authors study how P_ω , referred therein as the hybrid sampler, “inherits” other convergence properties from the kernels in \mathfrak{P} , such as geometric ergodicity, rate of convergence, etc. In this paper, we rather study the question whether or not the way (*i.e.* the distribution ω) to select the kernels in \mathfrak{P} affects the hybrid Markov kernel P_ω . This is known to be a challenging problem and [Andrieu \(2016\)](#) is probably the only literature available on this topic. The author carries out a thorough exploration of the hybrid Gibbs case, with $n = 2$ kernels, and compares the random-scan Gibbs sampler (RSGS) with the deterministic-update Gibbs sampler (DUGS), according to their asymptotic variance of empirical estimators.

Example 1 has shown that choosing the kernel in a locally meaningful way may lead to a substantial gain in terms of time to convergence. In this section, we introduce a class of Markov chain Monte Carlo algorithms (MCMC), referred to as *Locally informed MCMC* whose choice of transition kernel P_i at iteration t depends on the state X_t of the Markov chain. Define the function $\omega : \mathsf{X} \mapsto \Delta_n$. For any $i \in \{1, \dots, n\}$ and $x \in \mathsf{X}$, let us define $\omega_i(x)$ as the probability to select P_i as the next transition kernel if the Markov chain is at state $X = x$. More formally, the transition kernel of such a Markov chain is defined for any $(x, A) \in \mathsf{X} \times \mathcal{X}$ by

$$P_\omega(x, A) = \sum_{i=1}^n \omega_i(x) P_i(x, A). \quad (8)$$

For example, the case $d = n$ and $P_i(x, \cdot) = \pi(\cdot | x_{-i}) \delta_{x_{-i}}$ is a random-scan Gibbs sampler whose kernel selection distribution depends on the current state. However, such an algorithm is not necessarily π -invariant since

$$\pi P_\omega(A) = \sum_{i=1}^n \int \omega_i(x) \pi(dx) P_i(x, A)$$

does not, in general, equals $\pi(A)$. We stress that when ω is independent of the chain position, P_ω is π -invariant and corresponds to the case of Eq. (7).

We present a way to correct the algorithm P_ω so as to inherit the π -invariance from P_1, P_2, \dots, P_n . We refer to this type of algorithm as *Locally informed MCMC*, which is outlined in Algorithm 1.

Let P_ω^* be the transition kernel of the locally informed Markov chain described at Algorithm 1. It can be checked that P_ω^* writes:

$$\begin{aligned} P_\omega^*(x, A) &= \sum_{i=1}^n \omega_i(x) \left\{ \int_A P_i(x, dy) \alpha_i(x, y) + \delta_x(A) (1 - r_i(x)) \right\}, \\ r_i(x) &:= \int_{\mathsf{X}} P_i(x, dy) \alpha_i(x, y). \end{aligned} \quad (10)$$

Proposition 4. *Assume that for all $i \in \{1, \dots, n\}$, P_i is π -reversible, then for any choice of function $\omega : \mathsf{X} \rightarrow \Delta_n$, P_ω^* is π -reversible.*

Algorithm 1 Locally informed MCMC, transition $X_t \rightarrow X_{t+1}$

Require: $X_t = x \in \mathcal{X}$

1: draw $I \sim \omega(x) \rightsquigarrow i$

2: propose $\tilde{X} \sim P_i(x, \cdot) \rightsquigarrow \tilde{x}$ and set $X_{t+1} = \tilde{x}$ with probability

$$\alpha_i(x, \tilde{x}) = 1 \wedge \frac{\omega_i(\tilde{x})}{\omega_i(x)} \quad (9)$$

and $X_{t+1} = x$ otherwise.

Proof. Let ρ be a measure on $\mathcal{X} \otimes \mathcal{X}$ defined as $\rho(A, B) := \int_A \pi(dx) P_\omega^*(x, B)$ and $H : \mathcal{X}^2 \rightarrow \mathbb{R}$ a ρ -integrable test function. Establishing $\mathbb{E}_\rho\{H(X, Y)\} = \mathbb{E}_\rho\{H(Y, X)\}$ is sufficient to show that P_ω^* is π -reversible.

$$\begin{aligned} \mathbb{E}_\rho\{H(X, Y)\} &= \sum_{i=1}^n \iint_{\mathcal{X}} H(x, y) \pi(dx) P_i(x, dy) \{\omega_i(x) \wedge \omega_i(y)\} \\ &\quad + \sum_{i=1}^n \iint_{\mathcal{X}} H(x, y) \pi(dx) \delta_x(dy) \omega_i(x) (1 - r_i(x)) \\ &= \iint_{\mathcal{X}} H(x, y) \sum_{i=1}^n \omega_i(y) \pi(dy) P_i(y, dx) \{1 \wedge \omega_i(x)/\omega_i(y)\} \\ &\quad + \sum_{i=1}^n \iint_{\mathcal{X}} H(x, y) \pi(dy) \delta_y(dx) \omega_i(y) (1 - r_i(y)) \\ &= \iint_{\mathcal{X}} H(x, y) \pi(dy) P_\omega^*(y, dx) = \mathbb{E}_\rho\{H(Y, X)\}, \end{aligned}$$

where the second equality follows from the π -reversibility of P_i and the symmetry of the measure $\pi(dx)\delta_x(dy)$ on $\mathcal{X} \otimes \mathcal{X}$. \square

Since π -reversible Markov kernels are necessarily π -invariant, an immediate consequence of Proposition 4 is the following corollary.

Corollary 1. *Assume that for all $i \in \{1, \dots, n\}$, P_i is π -reversible, then for any choice of function $\omega : \mathcal{X} \rightarrow \Delta_n$, P_ω^* is π -invariant.*

Remark 2. *The locally informed kernel P_ω^* can be shown to be π -invariant using a probabilistic approach. Let $\mathcal{I} := \{1, \dots, n\}$ and its powerset $\mathcal{I} := \mathcal{P}(1, \dots, n)$. Consider the distribution $\bar{\pi}$ on $(\mathcal{X} \times \mathcal{I}, \mathcal{X} \otimes \mathcal{I})$ defined as*

$$\bar{\pi}(x, i) := \omega_i(x) \pi(x). \quad (11)$$

Define by $\{I_t, t \in \mathbb{N}\}$ the sequence of random variables drawn recursively at each iteration of Algorithm 1. Noting that $\bar{\pi}(i|x) = \omega_i(x)$, step (1) of Algorithm 1 can be regarded as a Gibbs update of I_t given $X_t = x$ and as such is $\bar{\pi}$ -invariant. Step (2) of Algorithm 1 can be regarded as a Metropolis-Hastings update of X_{t+1} given $(I_t, X_t) = (i, x)$. Indeed taking $P_i(x, \cdot)$ as the proposal kernel, step (2) consists in simulating $\tilde{X} \sim P_i(x, \cdot)$ and accepting/rejecting the proposal with the usual MH probability

$$1 \wedge \frac{\bar{\pi}(\tilde{X} | i) P_i(\tilde{X}, x)}{\bar{\pi}(x | i) P_i(x, \tilde{X})} = 1 \wedge \frac{\omega_i(\tilde{X}) \pi(\tilde{X}) P_i(\tilde{X}, x)}{\omega_i(x) \pi(x) P_i(x, \tilde{X})} = \alpha_i(x, \tilde{x}), \quad (12)$$

where $\alpha_i(x, \tilde{x})$ is defined at Eq. (9). The last equality holds because P_1, P_2, \dots are all π -reversible. This shows that a transition $(I_t, X_t) \rightarrow (I_{t+1}, X_{t+1})$ of Algorithm 1 is in fact a series of two $\bar{\pi}$ -invariant transitions and is thus $\bar{\pi}$ -invariant. Noting that π is the marginal of $\bar{\pi}$ with respect to X completes the proof.

Remark 3. The locally informed Markov chains used in Examples 1 and 2 are instances of Algorithm 1.

In the sequel, we refer to P_{ω^c} as the transition kernel defined in Eq. (8) where ω^c is constant on X , in contrast to P_{ω^*} where the function ω varies on X . One can wonder if the locally informed Markov chain (Algorithm 1) with kernel P_{ω^*} is more efficient than the corresponding uninformed one *i.e.* the chain with kernel P_{ω^c} . A first negative answer can be formulated as follows. Roughly speaking, the rejection step introduced at Step 2 of Algorithm 1 (see Eq. (9)) makes the locally informed chain less efficient in the sense of increasing the asymptotic variance of some Monte Carlo estimators, compared to the uninformed chain. The following Proposition establishes this result more formally.

Proposition 5. Let $f \in \mathcal{L}_0^2(\pi)$. For any π -reversible kernel P , define the asymptotic variance of the Monte carlo estimation of πf using the Markov chain $\{X_t, t \in \mathbb{N}\}$ with kernel P and $X_0 \sim \pi$ as

$$v(f, P) := \lim_{t \rightarrow \infty} \frac{1}{t} \text{var} \left\{ \sum_{k=0}^{t-1} f(X_k) \right\}. \quad (13)$$

Assume that

- (i) X is a continuous state space
- (ii) for all $i \in \{1, \dots, n\}$, P_i is absolutely continuous and π -reversible,
- (iii) the function f satisfies

$$\sum_{k=1}^{\infty} |\text{cov}\{f(X_0), f(X_k)\}| < \infty,$$

then we have

$$v(f, P_{\omega^*}) \geq v(f, P_{\omega^c}).$$

Proof. This proof follows from a slight adaptation of Theorem 4 in Maire et al. (2014). In the sequel, for notational simplicity we refer to $\{X_t, t \in \mathbb{N}\}$ as a Markov chain with $X_0 \sim \pi$ and transition kernel P_{ω^*} or P_{ω} , indifferently. In this proof we embed the Markov chain $\{X_t, t \in \mathbb{N}\}$ in the state space $(X \times \mathbb{I}, \mathcal{X} \otimes \mathcal{I})$ and consider the non-homogeneous chain of the type

$$\begin{aligned} \dots \longrightarrow \{X_k, I_k\} &\xrightarrow{Q} \{X_{k+1} = X_k, I_{k+1} \sim \omega(X_k) \rightsquigarrow i\} \\ &\xrightarrow{R} \{X_{k+2} \sim P_i(X_{k+1}, \cdot), I_{k+2} = i\} \longrightarrow \dots, \end{aligned} \quad (14)$$

where Q refers to the Gibbs update of I (Step 1 of Alg. 1) and R to the Metropolis-within-Gibbs update of X (Step 2 of Alg. 1). Recall that the Markov chain $\{(X_k, I_k), k \in \mathbb{N}\}$ admits $\bar{\pi}$ (11) as stationary distribution. Moreover, we note that both Q and R are $\bar{\pi}$ -reversible. In the context of the decomposition of P suggested in (14), let Q_{ω^*} and R_{ω^*} be the two kernels so that $P_{\omega^*} = Q_{\omega^*} R_{\omega^*}$ and similarly write $P_{\omega^c} = Q_{\omega^c} R_{\omega^c}$. Clearly, $R_{\omega^c} \succeq_P R_{\omega^*}$ *i.e.* for all $(x, i) \in X \times \mathbb{I}$ and $A \times B \in \mathcal{X} \otimes \mathcal{I}$,

$$R_{\omega^*}(x, i; A \times B \setminus \{x, i\}) = \int_A P_i(x, d\tilde{x}) \alpha_i(x, \tilde{x}) \leq P_i(x, A) = R_{\omega^c}(x, i; A \times B \setminus \{x, i\}).$$

A direct application of Theorem 4 of [Maire et al. \(2014\)](#) requires also to have $Q_{\omega^c} \succeq_P Q_\omega^*$. This holds if and only if for all $(x, i) \in \mathsf{X} \times \mathsf{I}$, $\omega_i^c < \omega_i(x)$. Apart from the trivial case where ω is constant, this is not true and thus $Q_{\omega^c} \not\succeq_P Q_\omega^*$. However, we note that the operator $Q_{\omega^c} - Q_\omega^*$ is null on $\mathcal{L}_0^2(\pi)$, since for any $Q \in \{Q_{\omega^c}, Q_\omega^*\}$

$$\begin{aligned} \langle f, Qf \rangle &= \sum_{i=1}^n \int_{\mathsf{X}} d\bar{\pi}(\mathrm{d}x, i) f(x) Qf(x, i), \\ &= \sum_{i=1}^n \sum_{j=1}^n \iint_{\mathsf{X}} \bar{\pi}(\mathrm{d}x, i) f(x) Q(x, i; \mathrm{d}\tilde{x}, j) f(\tilde{x}), \\ &= \int_{\mathsf{X}} \sum_{i=1}^n \bar{\pi}(\mathrm{d}x, i) f(x) \sum_{j=1}^n \omega_j(x) f(x) = \|f\|^2. \end{aligned}$$

At this stage we refer to the proof of Theorem 4 in [Maire et al. \(2014\)](#). The proof of Theorem 4 can be carried out in the same way, while relaxing the assumption $Q_{\omega^c} \succeq_P Q_\omega^*$ by $Q_{\omega^c} - Q_\omega^*$ being the null operator on $\mathcal{L}_0^2(\pi)$. More precisely, the last equation in the proof of Lemma 25 holds despite the fact that $Q_{\omega^c} \not\succeq_P Q_\omega^*$. Indeed, one of the term in the RHS of Lemma 25's last equation is null and the other is negative, because $R_{\omega^c} \succeq_P R_\omega^*$. This completes the proof. \square

Remark 4. *We cannot apply directly Theorem 4 from [Tierney \(1998\)](#) since $P_{\omega^c} \not\succeq_P P_\omega^*$ does not hold. Indeed for all $(x, A) \in \mathsf{X} \times \mathcal{X}$*

$$\begin{aligned} P_\omega^*(x, A \setminus \{x\}) &= \sum_{i=1}^n \omega_i(x) \int_{A \setminus \{x\}} P_i(x, \mathrm{d}y) \alpha_i(x, y) \\ &\leq \sum_{i=1}^n \omega_i^c P_i(x, A \setminus \{x\}) = P_{\omega^c}(x, A \setminus \{x\}) \\ &\Leftrightarrow \omega_i^c = \omega_i(x), \quad a.s. \end{aligned}$$

The more sophisticated framework of Theorem 4 from [Maire et al. \(2014\)](#) is needed to split the two types of update.

This shows that asymptotically, the locally informed construction suggested in [Algorithm 1](#) is worst than any uninformed strategy moving according to the same kernel collection \mathfrak{P} . However, as illustrated in [Section 2](#), for some sparse and filamentary distributions, the locally informed strategy yields to Markov chains with smaller mixing time. This is also the case in the following example, where theoretical mixing times are reported for the locally informed algorithm and its uninformed counterpart.

Example 4. *Let $\mathsf{X} = \{1, 2, 3\}^d$ with $d > 1$. Consider the generic distribution on X defined as follows:*

$$\pi \propto \begin{cases} 1 & x \in \mathcal{S}_d \cup \mathcal{T}_d \\ 100^{-d} & \text{otherwise} \end{cases} \quad (15)$$

where $(\mathcal{S}_d, \mathcal{T}_d)$ are subspaces of X of dimension 2 defined as follows:

$$\mathcal{S}_d := \{x \in \mathsf{X}, x_1 = \dots = x_{d-2} = 1\}, \quad \mathcal{T}_d := \{x \in \mathsf{X}, x_3 = \dots = x_d = 1\}.$$

A representation of π in the case $d = 3$ is given on the right panel of [Figure 4](#).

Since the full conditional distributions of π are known and X is a discrete space, one can use a Gibbs sampler to sample from π . In this case, the collection of kernels P_1, \dots, P_n corresponds to the full conditional distributions *i.e.* $n = d$ and for all $i \in$

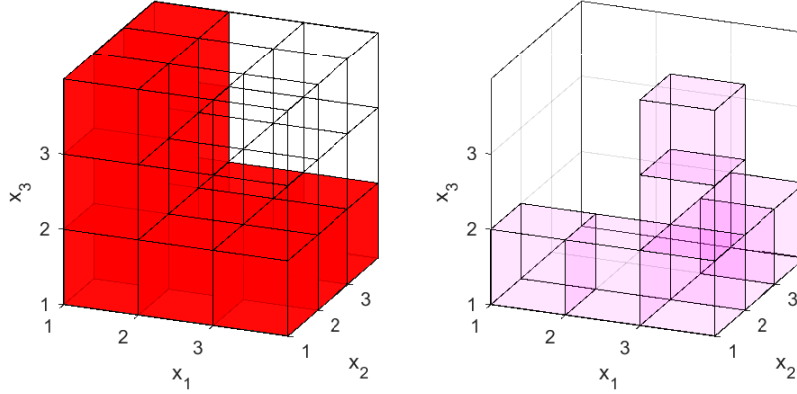


Figure 4: (Example 4, $d = 3$) Left panel: representation of π . Right panel: calculation of $\omega(x)$ where $x = (3, 1, 1)$. The weight $\omega_i(x)$ is proportional to the marginal $\pi_i(x)$ which is the sum of $\pi(x_{-i}, j)$ for $j = 1, 2, 3$ (states in purple), *i.e.* $\omega_1(x) = \omega_2(x) \propto 3 > \omega_3(x) \propto 1 + 10^{-6}$.

$\{1, \dots, d\}$, $A = \otimes_{i=1}^d A_i$, $P_i(x, A) = \delta_{x_{-i}}(A_{-i})\pi(A_i | x_{-i})$. We compare the speed of convergence of P_{ω^c} and P_{ω^*} with selection probabilities defined as:

$$\omega_i^c = 1/d, \quad \omega_i(x_{-i}) = \pi_i(x) := \sum_{j=1}^3 \pi(x_{1:i-1}, j, x_{i+1:d}). \quad (16)$$

The geometry of the problem leaves $\omega_i^c = 1/d$ as the only reasonable option for the constant selection probability. In contrast, when the function ω is allowed to be state dependent, it is designed so that the Markov chain attempts most of the time to move on either hyperplane where the probability mass of π is concentrated. The initial distribution μ is set as the dirac at state 1_d . Intuitively this corresponds to the case where one would assign the starting state of the Markov chain at a point $x_0 \in \mathcal{S}_d \cup \mathcal{T}_d$ found by a deterministic optimisation strategy so that it does not spend too much time wandering in $\mathbb{X} \setminus \{\mathcal{S}_d \cup \mathcal{T}_d\}$. We report in Figure 1 the total variation distances between π and the chain distribution for the two algorithms $\|\pi - \mu P_{\omega^c}^t\|$ and $\|\pi - \mu P_{\omega^*}^t\|$ for some $t \in \mathbb{N}$. We also provide the ϵ -mixing time $\tau(\epsilon) := \inf_{t \in \mathbb{N}} \{\|\pi - \mu P_{\omega^c}^t\| < \epsilon\}$ and $\tau^*(\epsilon) := \inf_{t \in \mathbb{N}} \{\|\pi - \mu P_{\omega^*}^t\| < \epsilon\}$, see Table 1. Since \mathbb{X} is discrete, all these quantities are exact.

		ϵ	1/4	0.1	0.01	0.001
$d = 2$	$\tau^*(\epsilon)$	2	3	5	6	
	$\tau(\epsilon)$	3	4	8	11	
$d = 5$	$\tau^*(\epsilon)$	4	6	11	16	
	$\tau(\epsilon)$	5	9	17	25	
$d = 8$	$\tau^*(\epsilon)$	5	8	14	21	
	$\tau(\epsilon)$	8	14	25	42	

Table 1: Mixing times for the locally informed and uninformed Markov chains.

In this example, the uninformed algorithm is penalized as it updates most of the time components that will keep the Markov chain at the same state. Indeed, when

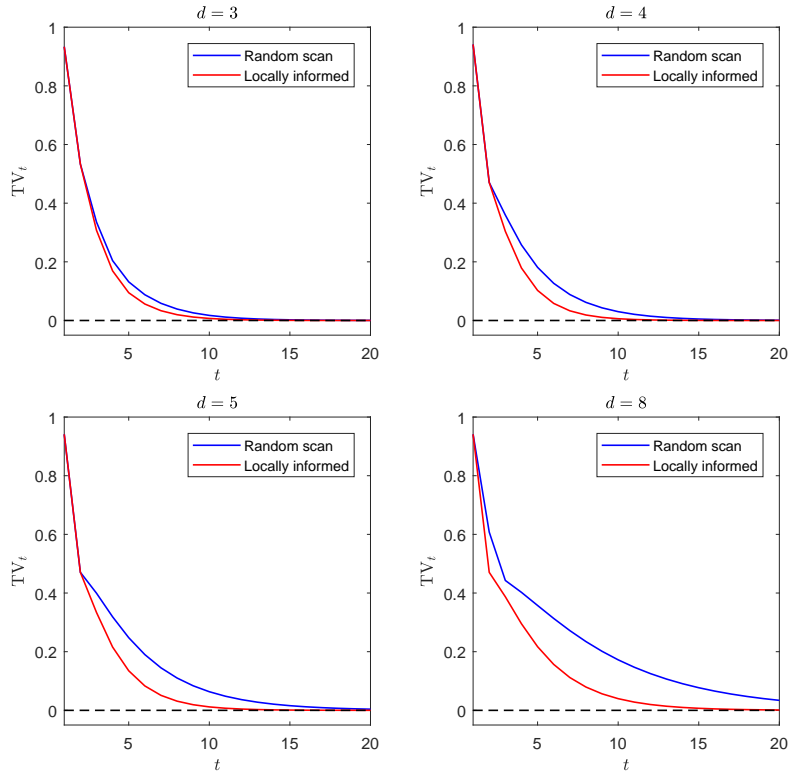


Figure 5: (Example 4) Convergence in TV for the non locally informed (RSGS) and locally informed Markov chains.

the chain is on $\mathcal{T}_d \cup \mathcal{S}_d$, then $1 - 2/d$ full conditional distributions have $1/(1 + 1/100^d)$ of their mass concentrated on the current state. In the same situation, the locally informed sampler will update components that will keep the Markov chain on $\mathcal{T}_d \cup \mathcal{S}_d$ but, with probability $1 - 1/d$, it will move to a different state. Note that Proposition 5 cannot be applied to compare the asymptotic variance of the two algorithms because \mathbf{X} is discrete.

5 A locally informed MCMC algorithm for Metropolis-Hastings kernels

In this section, we assume that \mathbf{X} is uncountable and that the collection of kernels \mathfrak{P} comprises exclusively Metropolis-Hastings kernels, *i.e.* for all $i \in \{1, \dots, n\}$, there exist an absolutely continuous Markov kernel Q_i , functions $\beta_i : \mathbf{X}^2 \rightarrow (0, 1)$ and $\varrho_i : \mathbf{X} \rightarrow (0, 1)$, such that for all $A \in \mathcal{X}$,

$$P_i(x, A) = \int_A Q_i(x, dy) \beta_i(x, y) + \delta_x(A)(1 - \varrho_i(x)), \quad (17)$$

where $\beta_i : \mathbf{X} \times \mathbf{X} \rightarrow (0, 1)$ is the acceptance probability defined as

$$\beta_i(x, y) = 1 \wedge \frac{\pi(y)Q_i(y, x)}{\pi(x)Q_i(x, y)} \quad \text{and} \quad \varrho_i(x) = \int_{\mathbf{X}} Q_i(x, dy) \beta_i(x, y).$$

By construction P_i is π -reversible. In this particular case, Algorithm 1 can be written as follows:

Algorithm 1 Locally informed MCMC for MH kernels, transition $X_k \rightarrow X_{k+1}$

Require: $X_k = x \in \mathsf{X}$

- 1: draw $I \sim \omega(x) \rightsquigarrow i$
- 2: propose $X \sim Q_i(x, \cdot) \rightsquigarrow \tilde{x}$
- 3: set $X_{k+1} = \tilde{x}$ with probability

$$\gamma_i(x, \tilde{x}) = \underbrace{\left\{ 1 \wedge \frac{\pi(\tilde{x})Q_i(\tilde{x}, x)}{\pi(x)Q_i(x, \tilde{x})} \right\}}_{\beta_i(x, \tilde{x})} \underbrace{\left\{ 1 \wedge \frac{\omega_i(\tilde{x})}{\omega_i(x)} \right\}}_{\alpha_i(x, \tilde{x})} \quad (18)$$

and $X_{k+1} = x$ otherwise.

Indeed, in the context of MH kernels, a proposal $X \sim Q_i$ is accepted only if it is accepted at the MH accept/reject step (cf. (17)) and at Step 2 of Algorithm 1. In this version of Alg. 1, an equivalent single accept/reject step (Step 3) is performed.

We introduce a second locally informed Markov chain $\{X_t, t \in \mathbb{N}\}$ relevant only when all the kernels P_1, \dots, P_n fall into the framework of Eq. (17).

Algorithm 2 A second locally informed MCMC for MH kernels, transition $X_t \rightarrow X_{t+1}$

Require: $X_t = x \in \mathsf{X}$

- 1: draw $I \sim \omega(x) \rightsquigarrow i$
- 2: propose $\tilde{X} \sim Q_i(x, \cdot) \rightsquigarrow \tilde{x}$ and set $X_{t+1} = \tilde{x}$ with probability

$$\bar{\gamma}_i(x, \tilde{x}) = 1 \wedge \frac{\pi(\tilde{x})Q_i(\tilde{x}, x)\omega_i(\tilde{x})}{\pi(x)Q_i(x, \tilde{x})\omega_i(x)} \quad (19)$$

and $X_{t+1} = x$ otherwise.

Proposition 6. *Let \bar{P}_ω be the transition kernel of the Markov chain $\{X_t, t \in \mathbb{N}\}$ described at Algorithm 2. Then, \bar{P}_ω is π -reversible.*

The proof is similar to that of Proposition 4.

Remark 5. *Similarly to Remark 2, the joint Markov chain $\{(X_t, I_t), t \in \mathbb{N}\}$ produced by Alg. 2 can be regarded as a Gibbs chain on the extended state space $(\mathsf{X} \times \mathbb{I}, \mathcal{X} \otimes \mathcal{I})$ targeting the distribution $\bar{\pi}$ defined in Eq. (11). Step (1) is a Gibbs update of I_t given $X_t = x$ and Step (2) is a Metropolis-within-Gibbs update of X_t given $I_t = i$. The only difference with Algorithm 1 is that the proposal distribution in this step is Q_i for Alg. 2, as opposed to P_i for Alg. 1.*

In the sequel, we will refer to as P_ω and \bar{P}_ω , the transition kernels corresponding to Algorithm 1 and Algorithm 2 respectively, regardless whether or not ω is uniform on X . In Algorithm 1, a proposal \tilde{X} can be rejected (1) because of the non-zero diagonal mass of P_i or (2) because of the rejection step necessary to keep the locally informed algorithm π -invariant. In contrast, a proposal \tilde{X} in Algorithm 2 faces only one accept/reject step. This naturally induces a Peskun ordering between the Markov kernels P_ω and \bar{P}_ω .

Proposition 7. Let P_1, \dots, P_n be n Metropolis-Hastings kernels and $f \in \mathcal{L}_0^2$. Let $\omega : \mathsf{X} \rightarrow \Delta_n$ be any weight function. Denote by P_ω and \bar{P}_ω the two transition kernels defined by Algorithms 1 and 2, respectively. Then we have

$$v(f, P_\omega) \geq v(f, \bar{P}_\omega), \quad (20)$$

where for any Markov kernel P and any $f \in \mathcal{L}^2(\pi)$, $v(f, P)$ is the asymptotic variance as defined in Eq. (13).

Proof. Contrarily to the proof of Proposition 3, we can directly compare the two kernels P_ω and \bar{P}_ω since the weight function ω is the same for both kernels. Note that for all $x \in \mathsf{X}$ and any $A \in \mathcal{X}$,

(i) the Markov subkernels associated to P_ω and \bar{P}_ω write

$$\begin{cases} P_\omega(x, A \setminus \{x\}) = \sum_{i=1}^n \omega_i(x) \int_A Q_i(x, dy) \gamma_i(x, y), \\ \bar{P}_\omega(x, A \setminus \{x\}) = \sum_{i=1}^n \omega_i(x) \int_A Q_i(x, dy) \bar{\gamma}_i(x, y) \end{cases}$$

(ii) for all $i \in \{1, \dots, n\}$ and for $(x, y) \in \mathsf{X}^2$,

$$\begin{aligned} \gamma_i(x, y) &= \left\{ 1 \wedge \frac{\pi(y)Q_i(y, x)}{\pi(x)Q_i(x, y)} \right\} \left\{ 1 \wedge \frac{\omega_i(y)}{\omega_i(x)} \right\} \\ &\leq 1 \wedge \frac{\pi(y)Q_i(y, x)\omega_i(y)}{\pi(x)Q_i(x, y)\omega_i(x)} = \bar{\gamma}_i(x, y), \end{aligned}$$

since for any positive real numbers (a, b) , $(1 \wedge a)(1 \wedge b) < 1 \wedge ab$.

Combining (i) and (ii), we obtain that $\bar{P}_\omega \succeq_P P_\omega$. Since P_ω and \bar{P}_ω are both π -reversible and $f \in \mathcal{L}_0^2(\pi)$, the inequality (20) follows by applying Theorem 4 from Tierney (1998). \square

Remark 6. Proposition 7 indicates that when P_1, \dots, P_n are MH kernels, the locally informed MCMC of Algorithm 2 should be preferred to Algorithm 1, when the efficiency is measured by the asymptotic variance.

Remark 7. Compared to the general case detailed in Section 3, Proposition 7 is less negative for locally informed Markov kernels. Indeed, contrarily to Proposition 5, the diagonal component of MH kernels ensures that the locally informed kernel from Algorithm 2 is not dominated by any uninformed algorithm using kernels in \mathfrak{P} , i.e. $P_{\omega^c} \not\prec_P \bar{P}_\omega$. This follows from the fact that for any $i \in \mathbb{N}$ and all $(x, y) \in \mathsf{X}^2$, the quantities $\bar{\gamma}_i(x, y)$ and $\beta_i(x, y)$ cannot be ordered.

6 Numerical Examples

In this section, we consider three general state space examples in which the distribution of interest can be seen as sparse and filamentary. We assume that a collection of n Metropolis-Hastings kernels P_1, \dots, P_n is available. Indeed, since the full conditional distributions of the models considered here are not straightforward, a Gibbs sampler cannot be implemented. With some abuse of notations, we will keep the acronym RSGS to refer to the algorithm which is sometimes known as ‘‘Metropolis-within-Gibbs’’. For each example, we clearly define the collection of available kernels and the weight function $\omega : \mathsf{X} \rightarrow (0, 1)^n$ used by the locally informed algorithms. Due to the symmetry of the models, the weight function for the RSGS algorithm is set as $\omega^c : \propto (1, 1, \dots, 1)$.

The non locally informed algorithm (RSGS) is compared with the two locally informed Markov algorithms (Alg. 1 or Alg. 2). The two strategies (i.e. locally informed

or not) are compared according to their time to convergence conditionally to some initial distribution μ_0 (*i.e.* in transient regime) and their asymptotic efficiency (*i.e.* in stationary regime) through the asymptotic variance of the empirical average of some test functions obtained using the sample path of Markov chains started at stationarity. More precisely,

- The convergence in distribution is assessed by estimating the Kullback-Leibler divergence (KL) between π and p_t , the Markov chain distribution at iteration t , conditionally on μ_0 . The KL divergence is estimated using a nearest neighbor entropy estimator, developed in [Chauveau and Vandekerkhove \(2013\)](#) and [Chauveau and Vandekerkhove \(2014\)](#).
- The asymptotic variances are estimated by simulating a large number of i.i.d. estimators of $\pi f \rightsquigarrow \{\widehat{\pi f}\}_1, \{\widehat{\pi f}\}_2, \dots$ each obtained through the simulation of a Markov chain trajectory started at stationary for T iterations. The asymptotic variance σ_f is thus estimated by

$$\widehat{\sigma}_f := T \widehat{\text{var}} \left(\{\widehat{\pi f}\}_1, \{\widehat{\pi f}\}_2, \dots \right),$$

where $\widehat{\text{var}}(x_1, x_2, \dots)$ denotes the unbiased variance estimator of the population (x_1, x_2, \dots) .

Example 5. Let π be the two-dimensional distribution (adapted from [Latuszynski et al. \(2013\)](#)) defined on the compact set $\mathsf{X} = [0, 1] \times [0, 1]$ by the density function with respect to the Lebesgue measure defined as:

$$\pi(x_1, x_2) := \frac{1}{2} \{ \varphi_N(x_1, x_2) + \varphi_N(x_2, x_1) \},$$

$$\varphi(x_1, x_2) : \propto x_1^{100} \{1 - \cos(10\pi x_2)\}.$$

The mass of π is concentrated near the subspaces $\{x_1 = 1\}$ and $\{x_2 = 1\}$ and varies in the neighborhood of those subspaces according to 5 sinusoids, see [Figure 6](#).

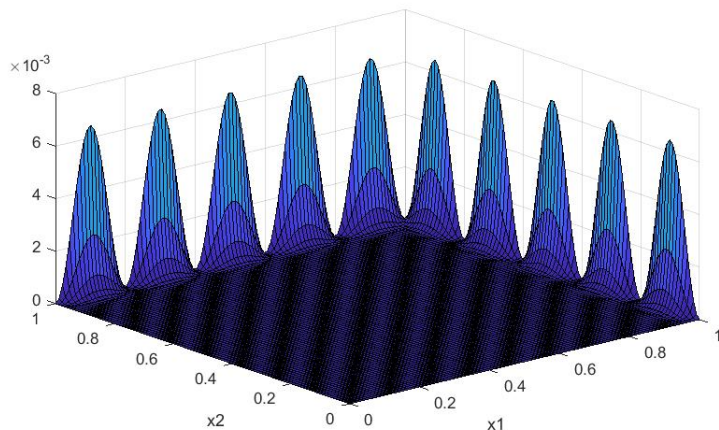


Figure 6: (Example 5) Plot of the density π .

The distribution π is sampled using RSGS and the two locally informed algorithms proposed in this paper ([Alg. 1](#) and [Alg. 2](#)).

Available kernels. There are $n = 4$ kernels available. P_1 freezes x_1 and moves x_2 according to a MH kernel with a truncated Gaussian proposal with standard deviation $\sigma_1 = 0.01$. P_2 operates in the same way as P_1 but with standard deviation $\sigma_2 = 1$. Finally, P_3 and P_4 are identical to P_1 and P_2 respectively but move x_1 and freeze x_2 .

Weight function RSGS uses a weight function defined as $\omega^c \propto (1, 1, 1, 1)$ while the two locally informed algorithms use

$$\omega(x) \propto \begin{cases} (x_1, 1 - x_1, x_2, 1 - x_2) & \text{if } \{x_1 < 0.9, x_2 < 0.9\}, \\ (x_1, 1 - x_1, x_1, 1 - x_1) & \text{if } \{x_1 > 0.9, x_2 < 0.9\}, \\ (x_2, 1 - x_2, x_2, 1 - x_2) & \text{if } \{x_1 < 0.9, x_2 > 0.9\}, \\ (1, 1, 1, 1) & \text{if } \{x_1 > 0.9, x_2 > 0.9\}. \end{cases}$$

This particular choice of $\omega(x)$ guarantees that large jumps are attempted with a probability that increases with the distance between x and the high density regions of π . It also ensures that the types of move in the high density regions are attempted according to the local topology of π . For instance, if the Markov chain is near the subspaces $\{x \in \mathbf{X}, x_1 = 1\}$, large moves in the x_2 direction are attempted so as to jump between the different modes of π and small moves in the x_1 direction are attempted to explore the tail of $\pi(\cdot | x_2)$.

Results In terms of distributional convergence, Figure 7 reports the estimated KL divergence between π and the three Markov chain distributions. It shows that even though the locally informed methods entropy decreases faster initially, the ϵ -mixing time seems to be quite the same for the algorithms for a small enough ϵ . Note that after $t = 100$ iterations, the convergence of Alg. 1 is clearly slower than the random scan method. Figure 8 illustrates the convergence of the Markov chains sample path average of a number of test functions (defined in Table 2) to their corresponding expectation. For this mode of convergence, the locally informed Algorithm 2 clearly shows an advantage over its two competitors. Indeed, after $t = 1,000$ iterations the bias is significantly lower when using Alg. 1 or RSGS. In terms of asymptotic efficiency, Table 2 summarizes our experiments. First, note that Alg. 2 is always more efficient than Alg. 1, a fact which illustrates Proposition 7. What was however unclear from the theoretical analysis is that, on this example and for those test functions, the locally informed methods (Algorithms 1 and 2) appear more efficient asymptotically than the non locally informed method (RSGS). Note that the asymptotic ordering between the RSGS and Algorithm 1 established at Proposition 5 does not apply to this example because P_1, \dots, P_4 are not absolutely continuous kernels. In particular, we observe that the asymptotic variances are significantly reduced when using Algorithm 2 instead of RSGS.

functions	RSGS	Alg. 1	Alg. 2
$f_1(x) := 1/(1 + x_1^{100})$	19.75	19.04	14.87
$f_2(x) := (1/x_1)\mathbf{1}_{\{0.4 < x_2 < 0.5\}}$	2.49	2.22	1.77
$f_3(x) := x_1/(1 + x_2)$	37.08	36.31	26.05
$f_4(x) := e^{-(x_1 - 0.8)^{10}}\mathbf{1}_{\{x_2 < 0.9\}}$	158.09	155.29	119.93

Table 2: (Example 5) Asymptotic variance for different functions $\bar{f} := f - \pi f \in \mathcal{L}_0^2(\pi)$ and three algorithms (RSGS and the two locally informed algorithms). Estimated from the simulation of 20,000 i.i.d. Markov chains for each algorithm ran for $n = 5,000$ iterations and initiated under π .

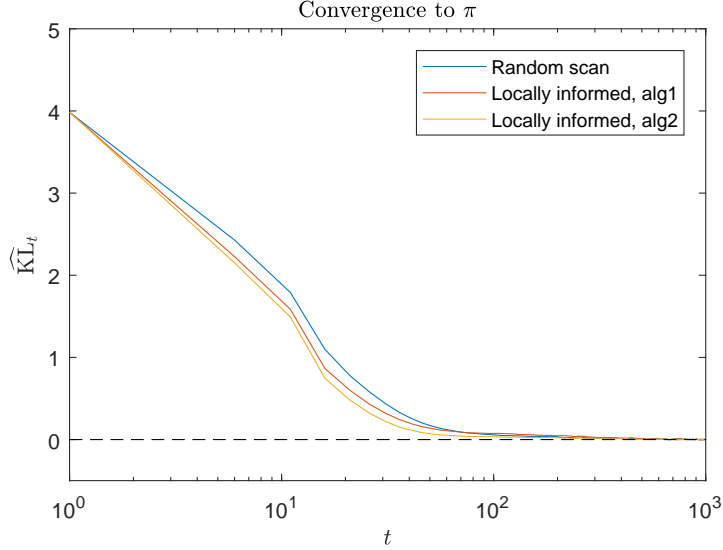


Figure 7: (Example 5) Convergence in distribution (measured in KL divergence) of the three Markov chains with initial distribution $\mu_0 = \mathcal{N}([0.95 \ 0.5], \text{Id}_2)$. Estimation based on 20,000 replications of the three Markov chains.

Example 6. Let π_θ be the distribution defined on $\mathsf{X} = \mathbb{R}^3$ as the following mixture of three Gaussians parameterized by $\theta > 0$:

$$\pi_\theta = (1/3) \left\{ \mathcal{N} \left(\begin{bmatrix} 0 \\ 2\sqrt{\theta} \\ 0 \end{bmatrix}, \Sigma_\theta^{(1)} \right) + \mathcal{N} \left(\begin{bmatrix} -2\sqrt{\theta} \\ 0 \\ 0 \end{bmatrix}, \Sigma_\theta^{(2)} \right) + \mathcal{N} \left(\begin{bmatrix} -2\sqrt{\theta} \\ -2\sqrt{\theta} \\ 2\sqrt{\theta} \end{bmatrix}, \Sigma_\theta^{(3)} \right) \right\}, \quad (21)$$

where for $(i, j, k) \in \{1, 2, 3\}^3$, $[\Sigma_\theta^{(i)}]_{j,k} := \mathbb{1}_{j=k}(1 + (\theta - 1)\mathbb{1}_{\{j=i\}})$. As θ increases, π_θ features a more pronounced sparse and filamentary structure, see Figure 9.

In this example, π is sampled using the RSGS algorithm and the locally informed algorithm (Alg. 2).

Available kernels Given the symmetry of π_θ (see Figure 9), two types of single-site update MH kernels with Gaussian random walk are considered: one with a large variance parameter σ_1^2 that allows a fast exploration of the edges and one with a smaller variance parameter σ_2^2 for local refinements on the boundaries of the filament or for directions orthogonal to it. In total, six MH kernels (two per direction) $P_\sigma^{(i)}$ with $\sigma \in \{\sigma_1, \sigma_2\}$ and $i \in \{1, 2, 3\}$ are considered.

Weight function The weight function gives larger probability to large moves in the edge direction and small moves to directions perpendicular to the edge. This is achieved by identifying which is the closest edge from the current state $x \in \mathsf{X}$. More

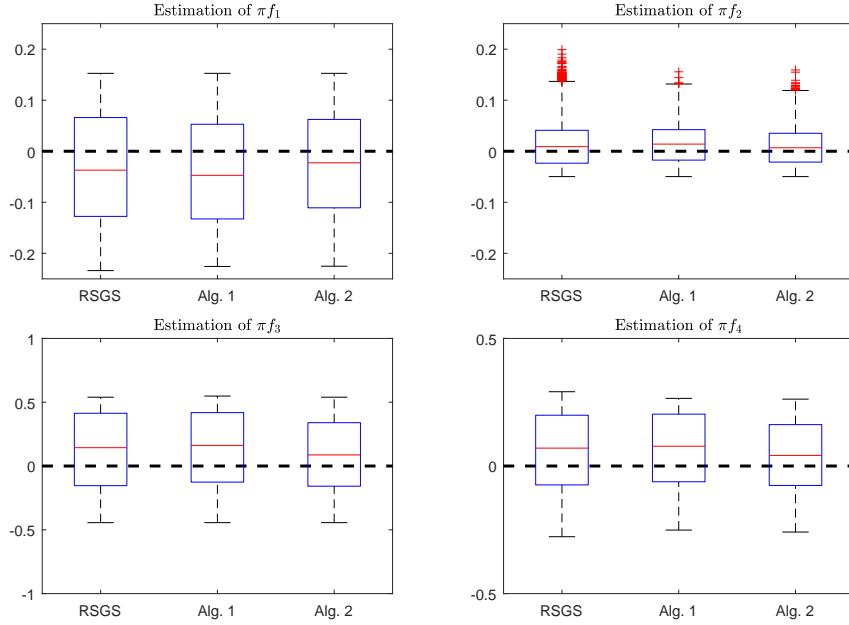


Figure 8: (Example 5) Convergence of the estimator of $\pi\bar{f}$, $\bar{f} := f - \pi f$, for different functions $f \in \{f_1, \dots, f_4\}$ and the three algorithms started with $\mu_0 = \mathcal{N}([0.95 \ 0.5], \text{Id}_2)$. The boxplots show the distribution of the estimator of πf for each method after $n = 1,000$ MCMC iterations and experiments were replicated 20,000 times.

formally, given some $\epsilon > 0$, we define the following functions

$$\omega_1(x) \propto \begin{pmatrix} 1 & \epsilon & \epsilon \\ 1/8 & 1/4 & 1/4 \end{pmatrix}, \quad \omega_2(x) \propto \begin{pmatrix} \epsilon & 1 & \epsilon \\ 1/4 & 1/8 & 1/4 \end{pmatrix},$$

$$\omega_3(x) \propto \begin{pmatrix} \epsilon & \epsilon & 1 \\ 1/4 & 1/4 & 1/8 \end{pmatrix}, \quad (22)$$

where the symbol \propto means that for all x , the matrix entries of $\omega_r(x)$ sum up to one. We refer to as $\{\phi_1, \phi_2, \phi_3\}$ the three Gaussian pdfs in the mixture π_θ (Eq. 21) and for all $x \in \mathbf{X}$ and $j \in \{1, 2, 3\}$, $\xi_j(x) \propto \phi_j(x)$ such that $\xi_1(x) + \xi_2(x) + \xi_3(x) = 1$. The weight function is defined by

$$\omega(x) := \sum_{k=1}^3 \xi_k(x) \omega_k(x). \quad (23)$$

In Eq. (23), $\omega(x)$ is a matrix whose entry $\omega_{i,j}(x)$ ($i \in \{1, 2\}$, $j \in \{1, 2, 3\}$) corresponds to the probability to draw from the kernel $P_{\sigma_j}^{(i)}$. In our experiments, we have used $\epsilon = 1/100$.

Results Contrarily to Example 5, π_θ is clearly a filamentary and sparse distribution, at least for large θ . Indeed, the variations of probability mass are smoother compared to the sinusoidal feature of π in Ex. 5. In fact, this example can be seen as the counterpart in $d = 3$ dimensions of the hypercube distribution described at Examples 1 (when

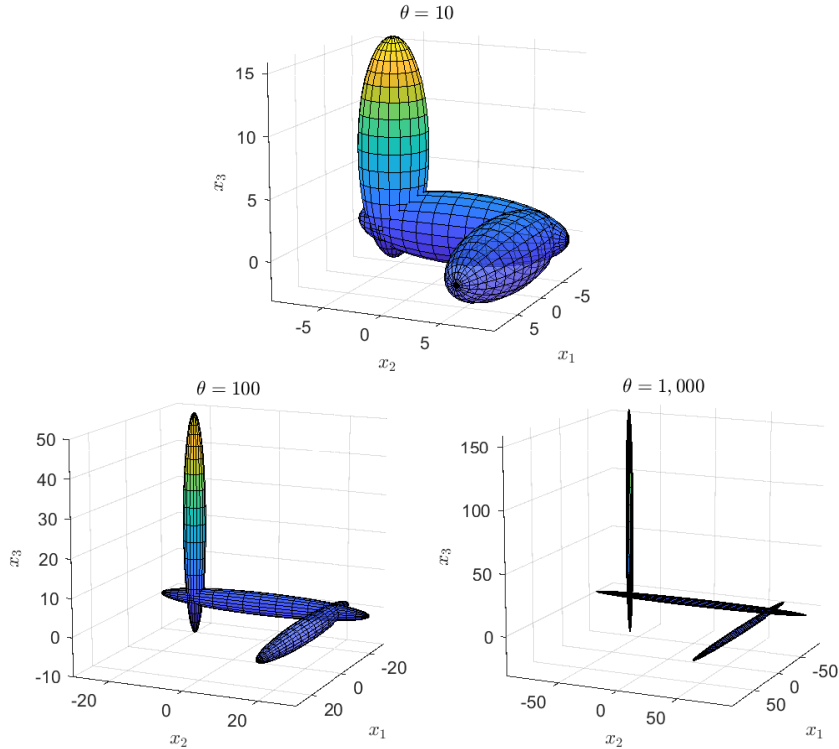


Figure 9: (Example 6) Representation of the probability density function π_θ , for three parameters $\theta \in \{10, 100, 1000\}$. The ellipsoids cover approximately 90% of the probability mass.

$\theta \rightarrow \infty$) and 2 (for a finite $\theta > 0$). Of course, the fact that \mathbf{X} is continuous in this example changes significantly the theory but one can wonder whether the results in terms of distributional convergence developed in Section 3 transposes to this situation. An empirical convergence analysis is carried out and Figure 10 reports the results. Interestingly, for large θ (e.g. $\theta \in \{500, 1000\}$), the convergence is sped up by a factor d when using the locally informed algorithm (Alg. 2) instead of the RSGS. Of course, the metric used in Figure 10 (KL) is different to that used in Proposition 2 (TV), but the speed up factor observed in this example is in line with the $d/2$ factor obtained at Propositions 1 and 2. We speculate that the factor 1/2 is here dropped as π_θ is not a uniform distribution on the filament as is π in Examples 1 and 2. For that reason, the relative speed of convergence between the two algorithms is not characterized by the speed at which the intersection area between two Gaussians is traversed (see Remark 1) and thus the relative speed of $1/d$ observed outside those areas prevails. Animations showing the convergence of p_t to π for the RSGS and the locally informed algorithm (Alg. 2) can be found online at http://maths.ucd.ie/~fmaire/MV18/ex6_theta10.gif for $\theta = 10$ (animations are also available for $\theta = 100$ and $\theta = 1,000$). In those animations, each figure contains 20,000 realizations of π (for the i.i.d. panel) and p_t for some $t > 0$ (for the MCMC panels). For the MCMC algorithms, $\mu_0 = \mathcal{N}([3\sqrt{\alpha} \ 2\sqrt{\alpha} \ 1], \text{Id}_3)$ was used as initial measure.

In terms of asymptotic efficiency, Table 3 reports the asymptotic variance related to the Monte Carlo estimator of πf , for four test functions $f \in \mathcal{L}_0^2(\pi)$ and for different

values of θ . Results seem to point to the same conclusion as Example 5, namely that the locally informed algorithm allows to reduce significantly the variance compared to the RSGS. However, what is interesting is that this ordering is reversed for larger noise levels (*e.g.* $\theta = 10$): as soon as π_θ loses its filamentary structure, RSGS becomes asymptotically more efficient than the locally informed algorithm. Putting this observation in the same picture as Figure 10, we conjecture the existence of a cut-off noise level θ^* : when $\theta > \theta^*$, the locally informed strategy dominates the random scan approach both in terms of distributional convergence and asymptotic efficiency, for a sufficiently large class of initial measures and test functions, and conversely when $\theta < \theta^*$.

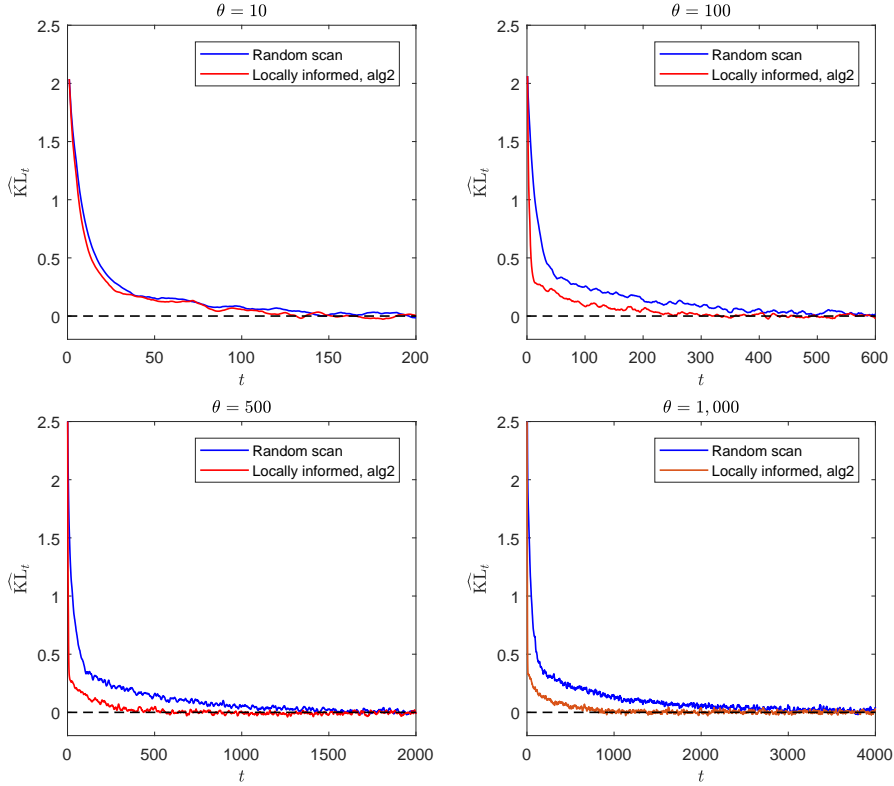


Figure 10: (Example 6) Convergence in distribution (measured in KL divergence) of the two Markov chains with initial distribution $\mu_0 = \mathcal{N}((3\sqrt{\alpha}, 2\sqrt{\alpha}, 1), \text{Id}_3)$, for $\theta \in \{10, 100, 500, 1000\}$. Estimation based on 1,000 replications of the two Markov chains. Note that the x-axis scale varies across plots.

Example 7. Let π_λ be the distribution of the random variable $X = Z + \zeta$ where $Z \sim \text{unif}(Z)$ and $\zeta = (\zeta_1, \zeta_2, \zeta_3)$. For all $i \in \{1, 2, 3\}$, the noise variable ζ_i has the same distribution as $\zeta_0 := (-1)^Y T$ with $Y \sim \text{ber}(1/2)$ and $T \sim \text{expo}(\lambda)$, for some noise parameter $\lambda > 0$. The subset $Z \subset X := \mathbb{R}^3$ is the union of two cylinders C_R and C_r having a fixed radius, R and r respectively, that are connected by a third cylinder C_ρ having a radius ρ that varies linearly in (r, R) . More precisely, C_R has a large radius R and a small height ℓ while C_r has a small radius r and a large height L . Note that ℓ and L are set such that $\text{vol}(C_r) = \text{vol}(C_\rho) = \text{vol}(C_R) = 1/3$. For a more formal definition,

$f(x)$	$\theta = 1,000$		$\theta = 100$		$\theta = 10$	
	RSGS	Alg. 2	RSGS	Alg. 2	RSGS	Alg. 2
$(x_1 + x_2)/(100 + x_3)$	1,034	350	35.61	33.97	1.15	2.40
$\mathbb{1}_{\{x_1 > x_2\}} e^{- x_3 }$	0.300	0.072	0.096	0.063	0.076	0.167
$\mathbb{1}_{\{x_1 > 2\sqrt{\theta}\}}$	0.831	0.120	0.210	0.114	0.115	0.193
$(x_1 + x_2)/2\sqrt{\theta} \vee 1$	25.23	7.16	6.43	5.61	2.20	4.23

Table 3: (Example 6) Asymptotic variance for different functions $\bar{f} := f - \pi f \in \mathcal{L}_0^2(\pi)$ and two algorithms (RSGS and the locally informed algorithm 2). Estimated from the simulation of 20,000 i.i.d. Markov chains for each algorithm ran for $n = 5,000$ iterations and initiated under π .

Z is parameterized by two positive numbers $(R, r) \in \mathbb{R}^2$ such that $r < R$ and is defined as:

$$Z := \left\{ (x_1, x_2, x_3) \in \mathbb{X} \mid \begin{aligned} & \left(\sqrt{x_2^2 + x_3^2} \leq R, -\ell < x_1 < 0 \right) \cup \\ & \left(\sqrt{x_2^2 + x_3^2} \leq R - x_1, 0 < x_1 < R - r \right) \cup \\ & \left(\sqrt{x_2^2 + x_3^2} \leq r, R - r < x_1 < R - r + L \right) \end{aligned} \right\}, \quad (24)$$

where $\ell := (R^2 - r^2)/(2R)$ and $L := (R^2 - r^2)/(2r)$. We have used $r = 0.05$ and $R = 1$ in the simulations. Illustrations of Z is given at Figure 11 and 10,000 i.i.d. draws from π_λ for different noise levels are plotted at Figure 12.

Even though deriving the analytical form of π_λ 's probability density function is not straightforward, it is tractable (as the convolution product $\text{unif}(Z) \otimes \text{dP}(\zeta \in \cdot)$) and therefore MCMC can be used to sample from π_λ . We compare the efficiency of the RSGS and the locally informed algorithm (Alg. 2) to sample from π_λ . Of course, in this example, sampling from π_λ can be achieved in a direct manner by adding noise to a point Z drawn uniformly at random in Z as suggested by the definition $X = Z + \zeta$. This scenario offers a controlled and tractable example aiming at mimicking distributions similar to π_λ but for which either the noise process and/or the boundary of Z is unknown. π_λ falls in the category of sparse and filamentary distribution since $\dim(\mathbb{X}) = 3$ while the two-third of the probability mass is concentrated either on a \mathcal{C}_R or \mathcal{C}_r which can be seen, at the limit, as a 2-dimensional subspace (a disk) and a 1-dimensional subspace of \mathbb{X} , respectively, see Figure 12.

Available kernels Taking into account the symmetry of π_λ , the RSGS algorithm takes turn (deterministically) in updating $x_1|(x_2, x_3)$ (move 1) and $(x_2, x_3)|x_1$ (move 2). For each type of update, the RSMwGS moves according to a collection of n MH kernels $P_1^{(i)}, \dots, P_n^{(i)}$ (for $i \in \{1, 2\}$). In particular, the proposal mechanism associated with $P_j^{(i)}$ can be described as follows. First, consider a set of n control points $\{\mathfrak{x}_1, \dots, \mathfrak{x}_n\} \in \mathbb{X}^n$ and define the following series of approximation for $j \in \{1, \dots, n\}$:

$$\hat{\pi}_j^{(1)} \approx \pi(\cdot | \mathfrak{x}_{2,j}, \mathfrak{x}_{3,j}), \quad \hat{\pi}_j^{(2)} \approx \pi(\cdot | \mathfrak{x}_{1,j}). \quad (25)$$

The construction of those approximations is discussed later. Now, assuming $x = (x_1, x_2, x_3)$ as current state, simulating a proposal is achieved as follows:

- With probability ϵ , a random walk type move is attempted,

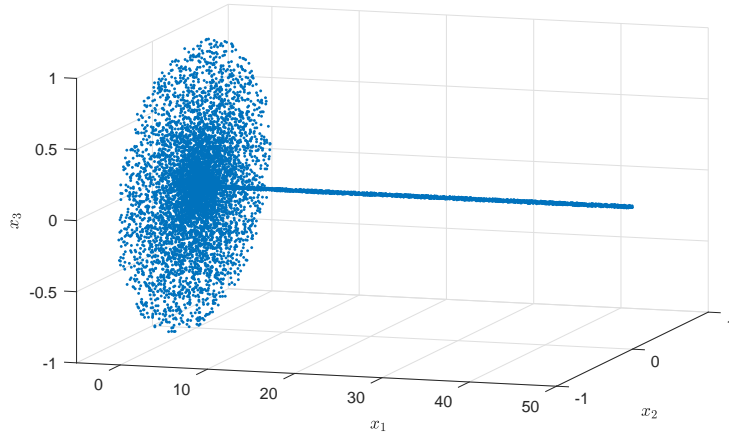


Figure 11: (Example 7) Points drawn uniformly at random in Z with $R = 1$ and $r = 1/100$.

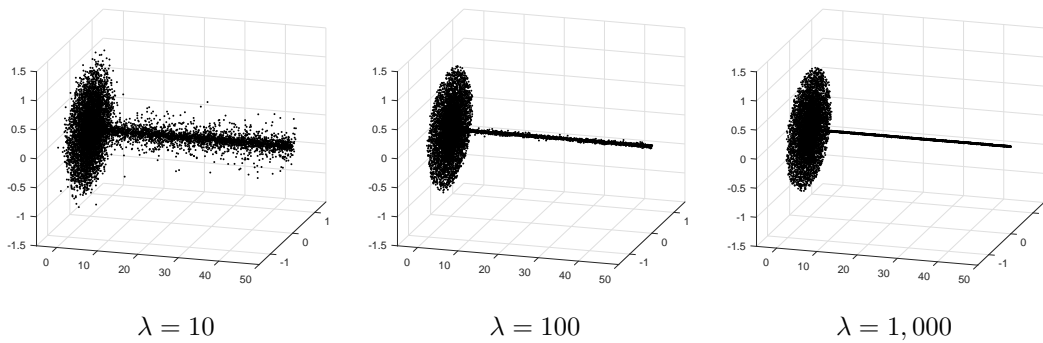


Figure 12: (Example 7) Realizations of $X \sim \pi_\lambda$ for different levels of noise.

- for move 1: propose $\tilde{X} = [x_1 + \sigma U, x_2, x_3]$ such that $U \sim \mathcal{N}(0, 1)$
- for move 2: propose $\tilde{X} = [x_1, R \cos(V), R \sin(V)]$ such that $R \sim \mathcal{N}(\sqrt{x_2^2 + x_3^2}, \sigma^2)$ and $V \sim \text{unif}(0, 2\pi)$
- With probability $1 - \epsilon$, an independent type move is attempted,
 - for move 1: propose $\tilde{X} = [\tilde{X}_1, x_2, x_3]$ with $\tilde{X}_1 \sim \hat{\pi}_j^{(1)}$
 - for move 2: propose $\tilde{X} = [x_1, \tilde{X}_2, \tilde{X}_3]$ with $(\tilde{X}_2, \tilde{X}_3) \sim \hat{\pi}_j^{(2)}$

Hence, with probability $1 - \epsilon$, the proposed state is drawn according to a proxy of the full conditional. Since RSGS draws the proposal kernel uniformly at random, there is a possibility that the proposal distribution, say $\hat{\pi}_j^{(2)}$, significantly differs from the full conditional $\pi(\cdot | x_1)$, a situation which is more likely to occur if $x_{1,j}$ is *far* from x_1 . At this stage, one may clearly see the benefit of a locally informed kernel selection: it can be designed so as to pick with high probability those kernels $P_j^{(2)}$ such that $x_{1,j}$ is close from x_1 . The construction of the approximations $\{\hat{\pi}_j^{(1)}, \hat{\pi}_j^{(2)}\}_{j=1}^n$ and the weight distribution used by the locally informed algorithm is now described.

Approximation of the full conditional distributions For type 1 move, it is defined as $\hat{\pi}_j^{(1)} := \text{unif}(-\ell, \mu_j)$ and for type 2 move, $\hat{\pi}_j^{(2)}$ is the distribution of the random vector $(R \cos(V), R \sin(V))$ with $R \sim \text{unif}(-\nu_j, \nu_j)$ and $V \sim \text{unif}(0, 2\pi)$. The constants $\{\mu_j, \nu_j\}_j$ are defined as follows:

$$\begin{cases} \mu_1 = 0, \nu_1 = R, \\ \mu_j = (R - r)(j - 1)/(n - 2), \nu_j = R - \mu_j \text{ for } j \in \{2, \dots, n - 2\}, \\ \mu_n = R - r + L, \nu_n = r. \end{cases} \quad (26)$$

In other words, the updated variables are drawn uniformly at random in \mathbb{Z} , conditionally on the control points $(x_{2,j}, x_{3,j})$ when x_1 is updated or $x_{1,j}$ when (x_2, x_3) is updated.

Weight function The weight function $\omega^{(i)}(x) := (\omega_1^{(i)}(x), \dots, \omega_n^{(i)}(x))$ is defined for the two types of move as follows:

$$\omega_j^{(1)}(x) : \begin{cases} = \delta_{j,n} & \text{if } \sqrt{x_2^2 + x_3^2} < r, \\ \propto 1 / \left| \sqrt{x_2^2 + x_3^2} - \sqrt{x_{2,j}^2 + x_{3,j}^2} \right| & \text{if } \sqrt{x_2^2 + x_3^2} \geq r, \end{cases} \quad (27)$$

$$\omega_j^{(2)}(x) : \begin{cases} = \delta_{j,1} & \text{if } x_1 < 0, \\ \propto 1 / |x_1 - x_{1,j}| & \text{if } 0 < x_1 < R - r, \\ = \delta_{j,n} & \text{if } x_1 > R - r. \end{cases} \quad (28)$$

The rationale of this design is here again to pick with high probability an independent proposal which is relevant for the local topology of π . In particular, Eq. (27) allows to pick $\hat{\pi}_j^{(1)}$ according to the distance between the chain and the control points $\{x_{2,j}, x_{3,j}\}$ while Eq. (28) picks $\hat{\pi}_j^{(2)}$ according to the distance between the chain and the control points $\{x_{1,j}\}$.

Results Starting from an initial distribution whose mass is located near the extremity of C_r , the convergence of the Markov chains simulated by RSGS and Algorithm 2 to π_λ (with four different values for the noise parameter λ) are compared at Figure 13. We again observe that for a large noise level (*e.g.* $\lambda = 10$), the RSGS converges faster than the locally informed Markov chain with the following pattern: Alg. 2 is faster at exploring most of the probability mass (within few iterations) before entering a slow converging mode that eventually sees RSGS catching up and entering an ϵ -ball

$f(x)$	$\lambda = 1,000$		$\lambda = 100$		$\lambda = 10$	
	RSGS	Alg. 2	RSGS	Alg. 2	RSGS	Alg. 2
$\rho(x)$	34.68	5.31	27.30	8.44	25.12	31.06
$x_1^{0.1}/(1 + \rho(x))$	103.4	15.26	80.85	15.38	29.34	26.10
$\mathbb{1}_{\{x_1 > R\}}$	184.3	25.7	147.39	25.15	57.39	39.89
$\mathbb{1}_{\{\rho(x) > 0.9R\}}$	2.22	0.46	2.69	6.63	29.47	41.19

Table 4: (Example 7) Asymptotic variance for different functions $\bar{f} := f - \pi f \in \mathcal{L}_0^2(\pi)$ and two algorithms (RSGS and the locally informed algorithm 2). Estimated from the simulation of 2,000 i.i.d. Markov chains for each algorithm ran for $n = 5,000$ iterations and started under π . In this Table, we have defined $\rho(x) := \sqrt{x_2^2 + x_3^2}$.

of π_λ (for some small $\epsilon > 0$) faster. Looking at scenarios with smaller noise level, the locally informed algorithm appears to converge (much) faster to a close neighborhood of π_λ than RSGS. However, as the precision of our experimental results is limited, it remains to be seen whether the rate of convergence is uniformly larger for Alg. 2 (*i.e.* for all $t > 0$) than for RSGS or if the locally informed algorithm will eventually enter a slow convergence mode (after some large t) that can simply be not perceived on the plots. Leaving theoretical considerations aside, the locally informed strategy is appealing as its empirical convergence from this initial distribution is 2, 3 and 5 times faster to RSGS, for $\lambda \in \{50, 100, 1000\}$ respectively. Animations of this scenario can be found online at http://maths.ucd.ie/~fmair/MV18/ex7_lambda10.gif for $\lambda = 10$ (also available for $\lambda = 100$ and $\lambda = 1,000$). Interestingly, the case $\lambda = 10$ shows the obvious difficulty for the locally informed algorithm to visit $X \setminus Z$. This is because by definition of ω (see Eq. (28)) moves outside Z will only be proposed with probability ϵ . More efficient strategies may exist but at the price of compromising the speed of convergence on Z . In terms of asymptotic efficiency, we observe similarly to Example 6 that the locally informed strategy can significantly reduce the asymptotic variance of Monte Carlo estimators for a diverse set of test functions, provided that the noise level is limited, *i.e.* that π_λ exhibits a filamentary structure.

7 Discussion

The main purpose of this paper was to investigate some properties of locally informed random scan MCMC. Given a fixed collection of π -reversible Markov kernels $\mathfrak{P} = P_1, \dots, P_n$ operating on (X, \mathcal{X}) , a locally informed algorithm simulates a Markov chain that moves, at each iteration, using a kernel drawn from the collection \mathfrak{P} and according to some state-dependent probability distribution ω . To the best of our knowledge, such a selection strategy has never been proposed in the literature. This contrasts with the significant research interest (Liu et al., 1994, 1995; Rosenthal, 1995; Roberts and Rosenthal, 1998a; Latuszynski et al., 2013; Andrieu, 2016) on random scan procedures in which the selection mechanism is state-independent, the random scan Gibbs sampler (RSGS) being a notorious example. A potential explanation is that if they are not carefully designed, locally informed algorithms can easily destroy the convergence properties of the kernels in \mathfrak{P} . We have proposed two locally informed algorithms in this paper: Algorithm 1 is applicable to any collection of π -reversible kernels \mathfrak{P} while Algorithm 2 needs the kernels in \mathfrak{P} to be Metropolis-Hastings type kernel. Locally informed algorithms are probably not always relevant: in fact we proved that Algorithm 1 is always less asymptotically efficient than any non-locally informed strategy making use of the same kernels (see Proposition 7) and that the latter may, in some

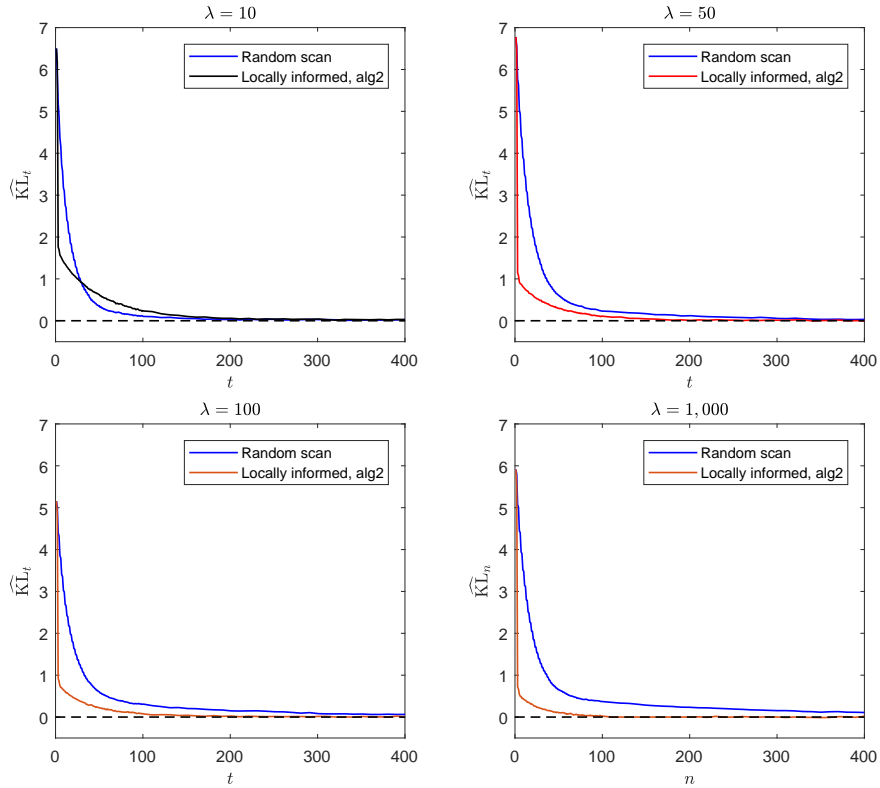


Figure 13: (Example 7) Convergence in distribution (measured in KL divergence) of the two Markov chains with initial distribution $\mu_0 = \mathcal{N}([R - r + L r/\sqrt{8} \ r/\sqrt{8}], 0.01\text{Id}_3)$, for $\lambda \in \{10, 50, 500, 1000\}$. Estimation based on 1,000 replications of the two Markov chains.

cases, enjoy better convergence properties than the former, see Proposition 3, Figures 2 ($p = 0.1$), 3, 10 ($\theta = 10$), 13 ($\lambda = 10$). Our point is that for a specific class of probability distributions that we refer to as sparse and filamentary, locally informed algorithms lead to Markov chains that converge faster to their stationary distribution and achieve a substantial auto-correlation reduction compared to their non locally informed counterpart. Even though at this stage, most of our conclusions are based on empirical observations, we believe that this research opens up a number of questions that may interest the Bayesian, machine learning and applied probability communities, among others. We conclude this paper by presenting some of them.

Practical questions While the purpose of this paper was essentially to expose some theoretical and empirical observations related to locally informed MCMC, we acknowledge that most of our examples assume that a significant amount of information on π is known *a priori*. In real life problems, it is unreasonable to take that knowledge as granted when implementing either Algorithm 1 or 2 and this leads to the following questions:

- *Design of \mathfrak{P}* . We have assumed that a collection of π -reversible kernels was already made available, *ex nihilo*. In practice, one first needs to design \mathfrak{P} in order to apply the RSGS or a locally informed algorithm. An easy route consists in defining \mathfrak{P} as a list of MH kernels with different proposals. Proposals may consist in local approximations (parametric or nonparametric) of π (or any full conditional distribution thereof), Gaussian random walk kernels with a collection of relevant covariance matrices (see *e.g.* Livingstone (2015)), etc. When the state space dimension is large, an idea is to apply a Principal Component Analysis algorithm to a dataset comprising of realizations from π (available for instance via a preliminary MH run), in order to identify relevant subspaces onto which MH kernels would operate.
- *Specification of ω* . When \mathfrak{P} is a collection of MH kernels, it is possible to define a time inhomogeneous weight function $\omega_t : \mathsf{X} \rightarrow \Delta_n$. Assume that at each iteration, random particles $\tilde{X}_{i,1}^{(t)}, \tilde{X}_{i,2}^{(t)}, \dots \sim_{\text{iid}} Q_i(x_t, \cdot)$ are drawn from the proposal Q_i (for $i \in \{1, \dots, n\}$) and are then used so that the weight function may be defined as:

$$\omega_{t,i}(x_t) \equiv \omega_{t,i}(x_t; \tilde{X}_{i,1}^{(t)}, \tilde{X}_{i,2}^{(t)}, \dots) \approx \mathbb{E}_{Q_i}(\pi(X) | x_t). \quad (29)$$

This design allows kernels attempting moves to local but reachable higher density regions to be promoted. Even though the locally informed Markov transition kernel is more complex to analyse when ω is defined as in Eq. (29), ω can be designed such that the locally informed algorithm remains π -stationary. It is for instance the case when an auxiliary particle is defined as $X_i^{(t)} = x_t + \eta_{t,i}$, where $\{\eta_{t,i}\}_{t,i}$ are exogenous variates. In such a scenario, the resulting locally informed Markov chain can be casted and analysed in a time inhomogeneous framework where each transition is conditioned by the auxiliary particles $\{\eta_{t,i}\}_{t,i}$, see *e.g.* Douc et al. (2004) for more details. Figure 14 reports the convergence of Algorithm 2 (in the context of Example 6) when ω is defined as in Eq. (29). The convergence is slightly slower than when the function ω defined in Example 6 (whose design required an extensive knowledge of π) is used but this fully automated choice of ω remains still very much competitive, especially compared to the RSGS.

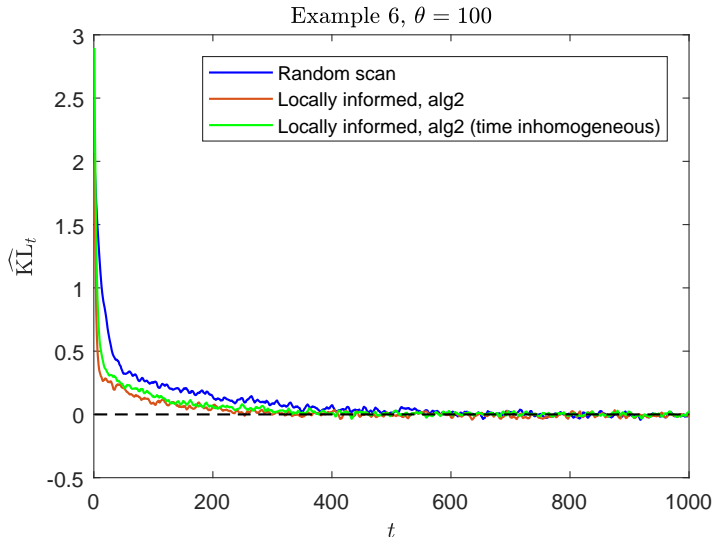


Figure 14: (Example 6): same experiment as reported in Figure 10 with in addition the locally informed algorithm (Alg. 2) implemented with ω defined as $\omega_{i,t}(x) := (1/L) \sum_{\ell=1}^L \pi_{\theta}(\tilde{X}_{i,\ell}^{(t)})$ and $\tilde{X}_{i,\ell}^{(t)} \sim_{\text{iid}} Q_i(x, \cdot)$ and $L = 100$, *i.e.* in the time inhomogeneous framework.

Theoretical considerations

- *Convergence on complementary subsets.* A much relevant question is to understand how the spectral analysis of Example 1 can be extended to situations where $\pi(\mathbf{X} \setminus \mathbf{Z}) > 0$, for instance when π is the mixture of two uniform distributions on \mathbf{Z} and $\mathbf{X} \setminus \mathbf{Z}$ with mixing probability $1 - p$ and p respectively (*i.e.* Example 2). Deriving such a result appears technically significantly more challenging since the simpler representation of the RSGS and the locally Markov chain on which the proof of Propositions 1 and 2 is based is no longer available. However, we mention the two following observations:
 - (i) When considering the restriction of the two algorithms to \mathbf{Z} , the locally informed MCMC is of order $d/2$ faster to converge than the RSGS (see Example 1).
 - (ii) When considering their restriction to $\mathbf{X} \setminus \mathbf{Z}$, the locally informed algorithm and the RSGS are identical and thus converge at the same speed.

It may appear paradoxical that considering the restriction of the two Markov chains to two complementary subsets of \mathbf{X} , the locally informed algorithm is faster or as fast than the RSGS, while the results of Example 2 show that the RSGS is in fact faster to converge than the locally informed algorithm when both Markov chains are studied on \mathbf{X} . Of course, a notable difference between the two algorithms is the frequency at which the chains switch between \mathbf{Z} and $\mathbf{X} \setminus \mathbf{Z}$. In the case of Example 2, it can readily be checked that $\Pr_{LI}(X_0 \in \mathbf{Z} \rightarrow X_1 \in \mathbf{X} \setminus \mathbf{Z}) = p \Pr_{RS}(X_0 \in \mathbf{Z} \rightarrow X_1 \in \mathbf{X} \setminus \mathbf{Z})$ and $\Pr_{LI}(X_0 \in \mathbf{X} \setminus \mathbf{Z} \rightarrow X_1 \in \mathbf{Z}) = p \Pr_{RS}(X_0 \in \mathbf{X} \setminus \mathbf{Z} \rightarrow X_1 \in \mathbf{Z})$, where \Pr_{RS} and \Pr_{LI} are the probability distributions generated by the RSGS and the locally informed algorithm respectively. Hence the locally informed algorithm is, by construction, more reluctant to jump on and off the fila-

mentary region Z than the RSGS. The question to address aims at understanding how transitions between $X \setminus Z$ and Z act as a bottleneck for the locally informed algorithm which eventually slows down its global convergence on X , compared to the RSGS. This point is illustrated in the context of Example 4 by the following animation, available at http://maths.ucd.ie/~fmaire/MV18/ex4_CV.gif. It shows that, when initiated by a distribution μ_0 that has its mass concentrated outside the filament, Algorithm 1 takes more time to jump on the filament while Algorithm 2 and the RSGS exhibits similar speed of convergence. Situations where a Markov process reaches equilibrium very quickly on two complementary subsets but very slowly globally have been deeply studied in chemical physics and especially in the context of protein dynamics. Protein dynamics are usually modeled as a Markov process that has essentially two macro states which correspond to the folded and unfolded conformations of the protein. In particular, those systems are characterized by a large spectral gap between the second and third eigenvalues, see Berezhkovskii and Szabo (2005); Buchete and Hummer (2008). By analogy, we conjecture that the spectrum of the locally informed Markov chain targeting a sparse and filamentary distribution in presence of noise typically features a first spectral gap of limited amplitude compared to its second spectral gap. It remains to be seen how the spectrum of the RSGS in the same situation is shifted compared to the noise-free case.

- *Mixing strategies?* Based on the previous observation, assessing the convergence speed of the locally informed algorithm can be analysed by considering a strategy that would mix a locally informed MCMC kernel (Algorithm 1 or 2) with an uninformed strategy (*e.g.* the RSGS). More formally, considering a collection of kernels \mathfrak{P} , a locally informed Markov kernel P_ω^* for some function $\omega : X \rightarrow \Delta_n$ (or \bar{P}_ω if \mathfrak{P} comprises only MH Markov kernels) and an uninformed Markov kernel P_{ω^c} for some vector $\omega^c \in \Delta_n$, define the mixed strategy

$$P_{\omega, \omega^c}^{(\varpi)} := \varpi P_\omega^* + (1 - \varpi) P_{\omega^c}, \quad \varpi \in (0, 1),$$

that moves according to the locally informed algorithm w.p. ϖ and the uninformed algorithm w.p. $1 - \varpi$. In this framework, the locally informed algorithm corresponds to $P_{\omega, \omega^c}^{(1)}$ and the uninformed algorithm to $P_{\omega, \omega^c}^{(0)}$. A variational analysis of the Markov kernel $P_{\omega, \omega^c}^{(\varpi)}$ (seen as a function of ϖ) could reveal the existence of some optimal mixing parameter ϖ^* , in the sense of minimizing the mixing time or the Markov chain autocorrelation. Our work suggests that, when π is *purely* filamentary and sparse (see *e.g.* the model of Eq. (1) with $\zeta = 0$ almost surely), $\varpi^* = 1$ while for situations where π deviates away from the filamentary and sparse framework, $\varpi^* < 1$. Our intuition is that for a number of sparse and filamentary distributions, the mixed strategy $P_{\omega, \omega^c}^{(\varpi)}$ implemented with a large parameter $\varpi < 1$ will inherit best of both worlds: fast convergence on the filament while overcoming the topological bottleneck at the boundary between Z and $X \setminus Z$.

8 Proofs

8.1 Proof of Proposition 1

Proof. We first recall some basic notions related to discrete Markov chains coupling. Let π be a distribution on (X, \mathcal{X}) and two π -invariant Markov chains $\{X_t\} := \{X_t, t \in \mathbb{N}\}$ and $\{X'_t\} := \{X'_t, t \in \mathbb{N}\}$ with the same transition matrix P . A joint process $\{\Gamma_t\} := \{(X_t, X'_t)\}$ defined on $(X \times X, \mathcal{X} \otimes \mathcal{X}, \mathbb{P})$ is referred to as a coupling of $\{X_t\}$ and

$\{X'_t\}$ if $\{\Gamma_t\}$ admits $\{X_t\}$ and $\{X'_t\}$ as marginal distributions. Defining the coupling time $\tau(\Gamma)$ as

$$\tau(\Gamma) := \inf_{t \in \mathbb{N}} \{X_t = X'_t\},$$

a useful property of coupled Markov chains, arising from the coupling inequality states that:

$$\|P^t(x, \cdot) - P^t(y, \cdot)\| \leq \mathbb{P}_{x,y}\{\tau > t\}, \quad (30)$$

where $\mathbb{P}_{x,y}$ is the probability distribution generated by the simulation of the coupled Markov chain $\{\Gamma_t\} = \{X_t, X'_t\}$ started at $\Gamma_0 = (x, y)$. In Eq. (30), we have used the shorthand notation τ for $\tau(\Gamma)$, noting however that a coupling time is relative to a specific coupling. Since we have

$$\sup_{x \in \mathsf{X}} \|P^t(x, \cdot) - \pi\| \leq \sup_{(x,y) \in \mathsf{X}^2} \|P^t(x, \cdot) - P^t(y, \cdot)\|, \quad (31)$$

combining Eqs. (30) and (31) shows that the coupling time distribution characterizes the Markov convergence. In particular, using Markov inequality, we have

$$\sup_{x \in \mathsf{X}} \|P^t(x, \cdot) - \pi\| \leq \frac{1}{t} \sup_{(x,y) \in \mathsf{X}^2} \mathbb{E}_{x,y}(\tau),$$

where $\mathbb{E}_{x,y}$ is the expectation under $\mathbb{P}_{x,y}$.

In this proof, for any quantity α relative to the random-scan Gibbs sampler (RSGS), the equivalent quantity related to the locally informed algorithm (Alg. 1) will be denoted as α^* . In particular, let \mathbb{P}^* be the probability distribution generated by Algorithm 1 and \mathbb{E}^* be the expectation operator under \mathbb{P}^* . Our proof shows that $\mathbb{E}_{x,y}^*(\tau) = (d/2)\mathbb{E}_{x,y}(\tau)$.

Without loss of generality, we order X such that the states $\{x_1, \dots, x_{1+d(n-1)}\}$ correspond to the filament (*i.e.* Z). We notice that the transition matrices M and M^* corresponding respectively to the RSGS and the locally informed sampler (Alg. 1) satisfy in this case:

$$M = \begin{bmatrix} P & 0 \\ A & B \end{bmatrix} \quad \text{and} \quad M^* = \begin{bmatrix} P^* & 0 \\ A^* & B^* \end{bmatrix}, \quad (32)$$

and clearly Z is an absorbing state. Assuming that both Markov chains start in Z , it is thus sufficient to analyse only the transition matrices P and P^* which are essentially the restriction of the Markov chains to Z . Let $\{X_t\}$ and $\{X_t^*\}$ be the two Markov chains generated by P and P^* respectively.

The first step of the proof consists in projecting the Markov chains $\{X_t\}$ and $\{X_t^*\}$ onto a smaller state space by lumping some states from Z together. Let us write Z as $\mathsf{Z} = \{\mathcal{V}_1, \mathcal{E}_1, \mathcal{V}_2, \mathcal{E}_2, \dots, \mathcal{E}_d, \mathcal{V}_{d+1}\}$ where \mathcal{V}_k and \mathcal{E}_k are respectively the k -th vertex and the k -th edge of the hypercube that belongs to Z such that $\mathcal{V}_k \cap \mathcal{E}_k = \{\emptyset\}$. The folded representation of the Markov chain $\{X_t\}$ with transition kernel P is the discrete time process $\{Y_t\}$ defined on $\mathsf{Y} = \{1, \dots, 2d+1\}$ as follows: if there is $k \in \{1, \dots, d+1\}$ such that $X_t = \mathcal{V}_k$, set $Y_t = 2k-1$ or if there is $k \in \{1, \dots, d\}$ such that $X_t \in \mathcal{E}_k$, set $Y_t = 2k$. In other words, $\{Y_t\}$ inherits the vertices from $\{X_t\}$ but aggregates together into a unique state, the states that are in between two consecutive vertices. The same mapping allows to define $\{Y_t^*\}$ as the *folded* version of the locally informed Markov chain $\{X_t^*\}$. An illustration of the folded Markov chains $\{Y_t\}$ and $\{Y_t^*\}$ is given in Figure 15, in the case where $d = 3$. In the following, we refer to as Q (resp. Q^*) the transition matrix of $\{Y_t\}$ (resp. $\{Y_t^*\}$).

The second step is to define a coupling for the two folded Markov chains $\{Y_t\}$ and $\{Y_t^*\}$. For simplicity, we only present the coupling for $\{Y_t\}$ but the same approach

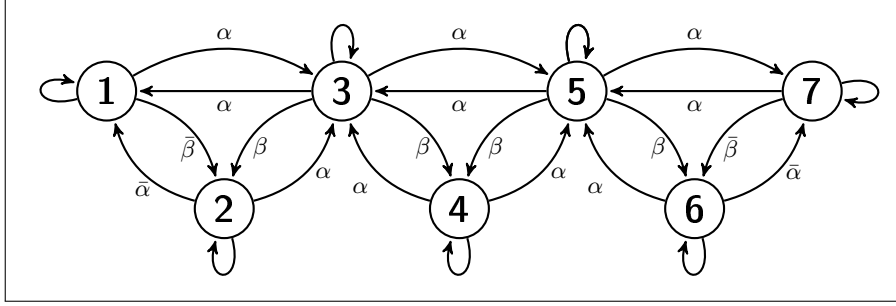


Figure 15: Projection on the folded space of the RSGS and locally informed Markov chains sampling from π , in the case where $d = 3$. The odd states correspond to vertices and the even ones to the aggregated states between two vertices. For the RSGS, the transition probabilities of the *folded* Markov chain $\{Y_t\}$ are $\alpha = \bar{\alpha} = 1/dn$ and $\beta = \bar{\beta} = \{1 - \frac{2}{n}\}/d$. For the locally informed algorithm, the transition probabilities of $\{Y_t^*\}$ are $\alpha^* = 1/2n$, $\bar{\alpha}^* = 1/n$, $\beta^* = (n - 2)/2n$ and $\bar{\beta}^* = (n - 2)/n$. For each state, the self loop indicate the probability to stay put, which equals one minus the sum of outwards probabilities.

is used for $\{Y_t^*\}$. Since there is an order on \mathcal{Y} , we consider the reflection coupling presented in Algorithm 3 that exploits the symmetry of the Markov chain. Clearly since $U \sim \text{unif}(0, 1)$ implies that $1 - U \sim \text{unif}(0, 1)$, the marginal chains satisfy $Y_t \sim Q^t(Y_0, \cdot)$ and $Y'_t \sim Q^t(Y'_0, \cdot)$ and the resulting discrete time process $\{(Y_t, Y'_t)\}$ jointly defined is a coupling of $\{Y_t\}$ and $\{Y'_t\}$. The coupling introduced in Algorithm 3, allows to derive the expected coupling time, *i.e.* the time at which the two Markov chains $\{Y_t\}$ and $\{Y'_t\}$ coalesce. By symmetry, the Markov chains coalesce necessarily when $Y_\tau = Y'_\tau = d + 1$. Therefore, denoting by \mathbb{E}_0° the expectation under the coupling $\{(Y_t, Y'_t)\}_t$ on $(\mathcal{Y} \times \mathcal{Y}, \mathcal{Y} \otimes \mathcal{Y})$ started at $Y_0 = 1$ and $Y'_0 = 2d + 1$, we have

$$\mathbb{E}_0^\circ(\tau) = \mathbb{E}_1^\circ(T_{d+1}) = \mathbb{E}_{2d+1}^\circ(T_{d+1}),$$

where for any $k \in \mathcal{Y}$, $T_k := \inf\{t > 0, Y_t = k\}$ and \mathbb{E}_k° denotes the expectation of the marginal Markov chain $\{Y_t\}$ started at $Y_0 = k$. The same coupling for the locally informed Markov chain yields $\mathbb{E}_0^{*\circ}(\tau) = \mathbb{E}_1^{*\circ}(T_{d+1})$. Central to this proof is the fact that a reflection coupling similar to Algorithm 3 exists for the Markov chains $\{X_t\}$ and $\{X_t^*\}$ and since the average time to reach the middle of the filament \mathcal{Z} when starting from one end is the same regardless whether the space is folded or not we have

$$\mathbb{E}_1^\circ(T_{d+1}) = \mathbb{E}_1(T_{d+1}), \tag{33}$$

which implies that $\mathbb{E}_0^\circ(\tau) = \mathbb{E}_0(\tau)$. The same argument holds for the locally informed Markov chain $\{X_t^*\}$ and its folded version $\{Y_t^*\}$.

Working on the folded space allows to derive $\mathbb{E}_1^\circ(T_{d+1})$ and $\mathbb{E}_1^{*\circ}(T_{d+1})$ in an easier way and this is the last part of the proof. We take d even so as to make the algebra more immediate. In this case, since $d + 1$ is odd, the state $d + 1$ corresponds to a vertex. A close examination of Figure 1 shows that $\mathbb{E}_1^\circ(T_{d+1})$ is the average time to absorption of a fictitious chain that would contain only the $d + 1$ first states, replacing the outwards connections of $d + 1$ by a self loop with probability 1. Denoting by Q_{d+1} the transition matrix of this fictitious chain, by Q_d the transition matrix of the d first transient states and by I_d the d -dimensional identity matrix, the matrix $I_d - Q_d$ is invertible and its inverse, often known as the fundamental matrix of Q_{d+1} , contains information related to the absorption time, see *e.g.* the Chapter 11 in [Grinstead and](#)

Algorithm 3 Reflection coupling on the hypercube

- 1: Initialise the two Markov chains with $Y_0 = 1$ and $Y'_0 = 2d + 1$
 - 2: Set $t = 0$, $Y = Y_0$ and $Y' = Y'_0$
 - 3: **while** $Y_t \neq Y'_t$ **do**
 - 4: Draw $U \sim_{\text{iid}} \text{unif}(0, 1)$ and set $U' = 1 - U$
 - 5: Define $\eta = \{\sum_{i=1}^j Q(Y, i)\}_{j=1}^d$ and $\eta' = \{\sum_{i=1}^j Q(Y', 2d + 1 - i)\}_{j=1}^d$
 - 6: Set $Y = 1 + \sum_{k=1}^{d-1} \mathbb{1}_{\eta_k < U}$ and $Y' = 1 + \sum_{k=1}^{d-1} \mathbb{1}_{\eta'_k < U'}$
 - 7: Set $t = t + 1$, $Y_t = Y$ and $Y'_t = Y'$
 - 8: **end while**
 - 9: Set $\tau = t$
 - 10: **for all** $t = \tau + 1, \tau + 2, \dots$ **do**
 - 11: Simulate Y_t using the steps (4)–(7) with $Y = Y_t$
 - 12: Set $Y'_t = Y_t$
 - 13: **end for**
-

[Snell \(2012\)](#). In particular, we have that for any $i < d$ starting position of the chain, then

$$\mathbb{E}_i^\diamond(T_{d+1}) = \{(I_d - Q_d)^{-1} \mathbf{1}_d\}_i,$$

where $\mathbf{1}_d$ denotes here the d -dimensional 1 vector. This implies that $\mathbb{E}_1^\diamond(T_{d+1})$ is simply the sum of the first row of $(I_d - Q_d)^{-1}$. It is possible to calculate analytically the fundamental matrix for each chain Q_{d+1} and Q_{d+1}^* and the proof follows from comparing each first row sum.

Using symbolic computation provided by Matlab, we found the following entries for the first row of the d -dimensional fundamental matrix of the RSGS

$$v_d = \frac{1}{\alpha(2\alpha + \beta)} (\beta, 2\alpha, 3\beta, 4\alpha, \dots, (d-1)\beta, d\alpha), \quad (34)$$

and

$$v_d^* = \frac{1}{\alpha(2\alpha^* + \beta^*)} (\beta^*, 2\alpha^*, \dots, (d-3)\beta^*, (d-2)\alpha^*, \alpha^*(2\alpha^* + \beta^*)\phi_d, \alpha^*(2\alpha^* + \beta^*)\psi_d),$$

where

$$\phi_d = \frac{2\beta^*}{\alpha^*\delta^*} \left\{ \left(\frac{3d}{2} - 1 \right) \alpha^* + (d-1)\beta^* \right\}, \quad \psi_d = \frac{1}{\delta^*} \{3d\alpha^* + (2d-1)\beta^*\},$$

and $\delta^* = 6\alpha^{*2} + 7\alpha^*\beta^* + 2\beta^{*2}$. Letting $d = 2p$ and using the fact that

$$\sum_{k=1}^{2p} k \mathbb{1}_{\{k \text{ is odd}\}} = p^2, \quad \sum_{k=1}^{2p} k \mathbb{1}_{\{k \text{ is even}\}} = p(p+1),$$

the sum of v_d 's elements is

$$\mathbb{E}_1^\diamond(T_d) = \frac{1}{\alpha(2\alpha + \beta)} \{\beta p^2 + \alpha p(p+1)\} = \frac{n-1}{4} d^3 + \frac{1}{2} d^2, \quad (35)$$

by definition of α and β . Using the same argument the sum of v_d^* 's elements is

$$\mathbb{E}_1^{*\diamond}(T_d) = \frac{n-1}{2} d^2 + (3-2n)d + 2(n-2) + \phi_d + \psi_d. \quad (36)$$

By straightforward algebra, we have

$$\phi_d + \psi_d = 2(n-1)d - 2(n-2),$$

which plugged into Eq. (36) yields

$$\mathbb{E}_1^{*\diamond}(T_d) = \frac{n-1}{2}d^2 + d. \quad (37)$$

The proof is completed by comparing Eqs. (35) and (37) and using Eq. (33). \square

8.2 Proof of Proposition 2

Proof. We consider a version of the locally informed kernel delayed by a factor $\lambda \in (0, 1)$:

$$P_\lambda^* = \lambda P^* + (1-\lambda)\text{Id}. \quad (38)$$

This proof shows that the convergence speed of the RSGS is similar to the locally informed algorithm, delayed by a factor $\lambda = 2/d$. The speed of convergence of π -reversible Markov kernels can be assessed by studying their spectral properties. Indeed, defining the spectral gap of a Markov kernel P as

$$\gamma(P) := 1 - \sup\{|\lambda|, \lambda \in \text{Sp}(P) \setminus \{1\}\},$$

where $\text{Sp}(P)$ is the spectrum of P , Proposition 2 from Rosenthal (2003) states that

$$\sup_{\mu \in \mathfrak{M}_1(\mathcal{Z})} \lim_{t \rightarrow \infty} \frac{1}{t} \log \|\mu P^t - \pi\| = \log(1 - \gamma(P)). \quad (39)$$

We recall that since P is a Markov operator, $\text{Sp}(P) \subset (-1, 1)$. Hence, the larger the spectral gap ($\gamma(P) \nearrow 1$), the faster the convergence. Getting the analytical expression of $\gamma(P)$ and $\gamma(P_\lambda^*)$ is challenging. Instead of calculating the eigenvectors of the transition matrices P and P_λ^* , we resort to the folded versions of those Markov chains in the same spirit as the proof of Proposition 1. Indeed, the resulting transition matrices on the folded space $\mathcal{Y} = \{1, 2, \dots, 2d+1\}$ are pentadiagonal and this facilitates the derivation of their spectrum.

We define the operators Γ and Ω that map \mathcal{Z} to \mathcal{Y} and \mathcal{Y} to \mathcal{Z} , respectively. Using the notation $\mathcal{Z} = \{\mathcal{V}_1, \mathcal{E}_1, \dots, \mathcal{V}_{d+1}\}$ defined in the proof of Proposition 1, Γ maps a state $x \in \mathcal{Z}$ to a step $y \in \mathcal{Y}$ as follows:

- If there exists $k \in \mathbb{N}$, such that $x = \mathcal{V}_k$, set $y = 2(k-1) + 1$.
- If there exists $k \in \mathbb{N}$, such that $x \in \mathcal{E}_k$, set $y = 2k$.

The operator Ω maps a state $y \in \mathcal{Y}$ to a step $x \in \mathcal{Z}$ as follows:

- If there exists $k \in \mathbb{N}$, such that $y = 2k + 1$, set $x = \mathcal{V}_{k+1}$.
- If there exists $k \in \mathbb{N}$, such that $y = 2k$, pick x uniformly at random in \mathcal{E}_k .

Hence, contrarily to Γ , Ω is a stochastic operator. More precisely, Ω and Γ are matrices such that $\Omega \in \mathcal{M}_{d(n-1)+1, 2d+1}((0, 1))$ and $\Gamma \in \mathcal{M}_{2d+1, d(n-1)+1}((0, 1))$ and their construction is detailed at Algorithm 4.

To circumvent calculating the eigenvalues of P and P_λ^* , a natural idea is to look at the spectrum of their equivalent transition kernels on the folded space \mathcal{Y} defined as

$$Q := \Gamma P \Omega \quad \text{and} \quad Q_\lambda^* := \Gamma P_\lambda^* \Omega \quad (40)$$

Algorithm 4 Construction of the mapping matrices

```

1: set  $\Omega_{1,\cdot} = \{\delta_{1,j}\}_{j \leq 2d+1}$  and  $\Gamma_{\cdot,1} = \{\delta_{1,j}\}_{j \leq 2d+1}$ 
2:  $k \leftarrow 2$ 
3: for all  $i = 2, \dots, d(n-1) + 1$  do
4:   if it exists  $\ell \geq 0$  s.t.  $i = \ell(n-1) + 1$  then
5:     set  $k \leftarrow k + 1$ 
6:     set  $\Omega_{i,\cdot} = \{\delta_{k,j}\}_{j \leq 2d+1}$  and  $\Gamma_{\cdot,i} = \{\delta_{k,j}\}_{j \leq 2d+1}$ 
7:     set  $k \leftarrow k + 1$ 
8:   else
9:     set  $\Omega_{i,\cdot} = \{\delta_{k,j}\}_{j \leq 2d+1}$  and  $\Gamma_{\cdot,i} = (1/(n-2))\{\delta_{k,j}\}_{j \leq 2d+1}$ 
10:  end if
11: end for

```

and illustrated at Figure 15 (in the case $\lambda = 0$). Unfortunately, those folded Markov chains cannot be directly used since $\text{Sp}(Q) \neq \text{Sp}(P)$ and $\text{Sp}(Q_\lambda^*) \neq \text{Sp}(P_\lambda^*)$. Indeed, it can be readily checked that

$$\text{Tr}(P) = 1 + (n-1)(d-1) \neq 2d-1 = \text{Tr}(Q) \quad (41)$$

and thus, should $\gamma(Q)$ and $\gamma(Q_\lambda^*)$ be analytically tractable, one could not call on to Eq. (39) to conclude the proof.

The trick is to consider the unfolded kernels stemming from Q and Q_λ^* and defined as

$$\bar{P} := \Omega Q \Gamma \quad \text{and} \quad \bar{P}_\lambda^* := \Omega Q_\lambda^* \Gamma. \quad (42)$$

Intuitively, while the dynamic of P is fundamentally on \mathbb{Z} , \bar{P} generates a process which fundamentally operates on \mathbb{Y} (via Q) and which is then projected back to \mathbb{Z} . It can be readily checked that $P \neq \bar{P}$ and $P_\lambda^* \neq \bar{P}_\lambda^*$. In particular, for any $(i, j) \in \mathcal{E}_k^2$ such that $i \neq j$, $P(i, i) \neq P(i, j)$ while $\bar{P}(i, i) = \bar{P}(i, j)$. The same point can be made about P_λ^* and \bar{P}_λ^* . Nevertheless, \bar{P} and \bar{P}_λ^* are still useful for our analysis. Remarkably, Lemma 1 shows that for any $t > 0$ and any starting point x in the set of vertices, we have

$$\|\delta_x P^t - \pi\| = \|\delta_x \bar{P}^t - \pi\| \quad \text{and} \quad \|\delta_x P_\lambda^{*t} - \pi\| = \|\delta_x \bar{P}_\lambda^{*t} - \pi\|. \quad (43)$$

As a consequence, when assessing the efficiency of P one can equivalently study \bar{P} and similarly for P^* with \bar{P}_λ^* . It can be checked that \bar{P} and \bar{P}_λ^* are symmetric and since π is the uniform distribution on \mathbb{Z} , both Markov kernels are thus π -reversible. Hence, combining Eq. (43) and Proposition 2 from Rosenthal (2003) applied to \bar{P} and \bar{P}_λ^* shows that the relative speed of convergence of the RSGS and the delayed locally informed MCMC can be assessed by comparing $\text{Sp}(\bar{P})$ and $\text{Sp}(\bar{P}_\lambda^*)$. Lemma 3 proves that $\gamma(\bar{P}) = \gamma(Q)$ and $\gamma(\bar{P}_\lambda^*) = \gamma(Q_\lambda^*)$. Lemma 4 completes the proof by showing that $\gamma(Q) = \gamma(Q_{2/d}^*)$. □

8.3 Proof of Proposition 3

Proof. In the context of Proposition 3, let P be the transition matrix associated to uninformed strategy. The matrix P can be seen as a plain Metropolis-Hastings with proposal $Q(i, j) := (1/2)\mathbb{1}_{i \neq j}$ and acceptance probability $\alpha(i, j) = 1 \wedge \pi(j)/\pi(i)$ that

guarantees the Markov chain to be π -reversible. By straightforward algebra, we have:

$$P = \frac{\mathbb{1}_{\{p \leq 1/3\}}}{2(1-p)} \begin{pmatrix} 1-3p & 1-p & 2p \\ 1-p & 1-3p & 2p \\ 1-p & 1-p & 0 \end{pmatrix} + \frac{\mathbb{1}_{\{p > 1/3\}}}{4p} \begin{pmatrix} 0 & 2p & 2p \\ 2p & 0 & 2p \\ 1-p & 1-p & 2(3p-1) \end{pmatrix}.$$

Note that $\lambda_0 = 1 \in \text{Sp}(P)$ since by construction P admits a stationary distribution. The general method to derive the two other eigenvalues $(\lambda_1, \lambda_2) \in \text{Sp}(P)$ (we use the convention $\lambda_1 \geq \lambda_2$) involves calculating the trace and the determinant of P . We note that

$$\begin{cases} 1 + \lambda_1 + \lambda_2 = \text{tr}(P) \\ \lambda_1 \lambda_2 = \det(P) \end{cases} \quad (44)$$

and as a consequence (λ_1, λ_2) are the solution of the quadratic equation

$$\lambda^2 - \{\text{tr}(P) - 1\}\lambda + \det(P) = 0.$$

Solving this equation yields the following spectrum

$$\sigma(p) = \mathbb{1}_{\{p \leq 1/3\}} \left\{ 1, \frac{-p}{1-p}, \frac{-p}{1-p} \right\} + \mathbb{1}_{\{p > 1/3\}} \left\{ 1, 1 - \frac{1}{2p}, -\frac{1}{2} \right\}$$

and the spectral gap is thus

$$\gamma(p) = \mathbb{1}_{\{p \leq 1/3\}} \frac{1-2p}{1-p} + \mathbb{1}_{\{p > 1/3\}} \frac{1}{p}.$$

We now consider the transition kernel P^* of the locally informed Markov chains. It corresponds to Algorithm 2 implemented with proposals Q_1 and Q_2 given at Eq. (6) and the weight function $\omega(i) \propto (\pi(\inf\{X \setminus \{i\}\}), \pi(\sup\{X \setminus \{i\}\}))$ for any $i \in X$. By straightforward algebra, we have:

$$P^* = \frac{\mathbb{1}_{\{p \leq 1/3\}}}{2(1-p)(1+p)} \begin{pmatrix} 2p(1-3p) & 2(1-p)^2 & 2p(1+p) \\ 2(1-p)^2 & 2p(1-3p) & 2p(1+p) \\ (1-p)(1+p) & (1-p)(1+p) & 0 \end{pmatrix} + \frac{\mathbb{1}_{\{p > 1/3\}}}{(1+p)} \begin{pmatrix} 0 & 1-p & 2p \\ 1-p & 0 & 2p \\ 1-p & 1-p & 0 \end{pmatrix},$$

and the spectrum is given by

$$\sigma^*(p) = \mathbb{1}_{\{p \leq 1/3\}} \left\{ 1, -\frac{p}{1-p}, -\frac{1-3p+4p^2}{1-p^2} \right\} + \mathbb{1}_{\{p > 1/3\}} \left\{ 1, \frac{p-1}{p+1}, \frac{p-1}{p+1} \right\}.$$

The spectral gap is thus

$$\gamma^*(p) = \frac{p(3-5p)}{1-p^2} \mathbb{1}_{\{p \leq 1/3\}} + \frac{2p}{1+p} \mathbb{1}_{\{p > 1/3\}},$$

which completes the proof. \square

9 Technical Lemmas

Lemma 1. *Let P be the transition matrix of the RSGS, Q its equivalent representation on the folded state space and Ω and Γ be the two mapping matrices defined at Algorithm 4 and let $\bar{P} := \Omega Q \Gamma$ and $\bar{P}_\lambda^* := \Omega Q^*_\lambda \Gamma$. Then we have for $x = (1, 1, \dots, 1, 1)$ and all $t > 0$*

$$\delta_x P^t = \delta_x \bar{P}^t. \quad (45)$$

Similarly for the locally informed algorithm, we have for all $t > 0$

$$\delta_x P_\lambda^{*t} = \delta_x \bar{P}_\lambda^{*t}. \quad (46)$$

Proof of Lemma 1. We prove Eqs. (45) and (46) by induction. For notational simplicity, we present the proof for $\lambda = 1$, i.e. $\bar{P}_\lambda^* \equiv \bar{P}^*$. We first establish Eq. (45). We use the notation of Proof of Proposition 1 and let $\mathcal{V} := \{\mathcal{V}_1, \dots, \mathcal{V}_{d+1}\}$. The initialisation follows from noting that $P(x, \cdot) = \bar{P}(x, \cdot)$, for any $x \in \mathcal{V}$. Now, assume that $\delta_x P^t = \delta_x \bar{P}^t$ and note that

$$\begin{aligned} \delta_x P^{t+1} &= \sum_{i \in \mathcal{V}} P^t(x, i) P(i, \cdot) + \sum_{i \in \mathcal{E}} P^t(x, i) P(i, \cdot), \\ &= \sum_{i \in \mathcal{V}} \bar{P}^t(x, i) P(i, \cdot) + \sum_{i \in \mathcal{E}} \bar{P}^t(x, i) P(i, \cdot), \\ &= \sum_{i \in \mathcal{V}} \bar{P}^t(x, i) \bar{P}(i, \cdot) + \sum_{k=1}^d \sum_{i \in \mathcal{E}_k} \bar{P}^t(x, i) P(i, \cdot), \end{aligned} \quad (47)$$

where the first line comes from the recursion assumption and the second follows from the initialisation stage. The second term in the last line of Eq. (47) requires a special attention. In particular, Lemma 2 shows that for all $x \in \mathcal{V}$ and any edge state i , $\bar{P}^t(x, i)$ depends only on i through the edge it belongs to. In other words, for all $k \in \{1, \dots, d\}$, there exists a function ρ_k^t such that $\bar{P}^t(x, i) = \rho_k^t(x)$ for all $i \in \mathcal{E}_k$ and all $x \in \mathcal{V}$. Plugging this into Eq. (47) yields

$$\delta_x P^{t+1} = \sum_{i \in \mathcal{V}} \bar{P}^t(x, i) \bar{P}(i, \cdot) + \sum_{k=1}^d \rho_k^t(x) \sum_{i \in \mathcal{E}_k} \bar{P}(i, \cdot). \quad (48)$$

Finally, we note that

$$\sum_{i \in \mathcal{E}_k} P(i, \cdot) = \sum_{i \in \mathcal{E}_k} \bar{P}(i, \cdot). \quad (49)$$

Indeed, by straightforward algebra, denoting V_{k-1} and V_k the adjacent vertices of \mathcal{E}_k , it can be readily checked that $\sum_{i \in \mathcal{E}_k} P(i, j) = \sum_{i \in \mathcal{E}_k} \bar{P}(i, j) = \{(n-2)/dn\} \mathbb{1}_{j \in \{V_{k-1}, V_k\}} + (1 - 2/dn) \mathbb{1}_{j \in \mathcal{E}_k}$. Combining Eqs. (48) and (49) finally yields

$$\begin{aligned} \delta_x P^{t+1} &= \sum_{i \in \mathcal{V}} \bar{P}^t(x, i) \bar{P}(i, \cdot) + \sum_{k=1}^d \rho_k^t(x) \sum_{i \in \mathcal{E}_k} \bar{P}(i, \cdot) \\ &= \sum_{i \in \mathcal{V}} \bar{P}^t(x, i) \bar{P}(i, \cdot) + \sum_{i \in \mathcal{E}} \bar{P}(x, i)^t \bar{P}(i, \cdot) = \delta_x \bar{P}^{t+1}, \end{aligned}$$

which completes the first part of the proof. To prove Eq. (46), we note that the initialisation is straightforward since there is a one-to-one mapping on \mathcal{V} between the folded and unfolded representation. The induction is concluded by applying the same reasoning, noting that Lemma 2 holds for \bar{P}^* also and that

$$\sum_{i \in \mathcal{E}_k} P^*(i, \cdot) = \sum_{i \in \mathcal{E}_k} \bar{P}^*(i, \cdot). \quad (50)$$

Indeed,

- for $k = 1$,
 - $\sum_{i \in \mathcal{E}_1} P^*(i, j) = (n - 2)/n = \sum_{i \in \mathcal{E}_1} \bar{P}^*(i, j)$ if $j = \mathcal{V}_1$,
 - $\sum_{i \in \mathcal{E}_1} P^*(i, j) = 1 - 3/2n = \sum_{i \in \mathcal{E}_1} \bar{P}^*(i, j)$ if $j \in \mathcal{E}_1$,
 - $\sum_{i \in \mathcal{E}_1} P^*(i, j) = (n - 2)/2n = \sum_{i \in \mathcal{E}_1} \bar{P}^*(i, j)$ if $j = \mathcal{V}_2$,
 - $\sum_{i \in \mathcal{E}_1} P^*(i, j) = 0 = \sum_{i \in \mathcal{E}_1} \bar{P}^*(i, j)$ for any $j \in \mathcal{V} \setminus \{\mathcal{V}_1, \mathcal{E}_1, \mathcal{V}_2\}$,
- for $1 < k < d$,
 - $\sum_{i \in \mathcal{E}_k} P^*(i, j) = (n - 2)/2n = \sum_{i \in \mathcal{E}_k} \bar{P}^*(i, j)$ if $j \in \{\mathcal{V}_k, \mathcal{V}_{k+1}\}$,
 - $\sum_{i \in \mathcal{E}_k} P^*(i, j) = 1 - 1/n = \sum_{i \in \mathcal{E}_k} \bar{P}^*(i, j)$ if $j \in \mathcal{E}_k$,
 - $\sum_{i \in \mathcal{E}_k} P^*(i, j) = 0 = \sum_{i \in \mathcal{E}_k} \bar{P}^*(i, j)$ for any $j \in \mathcal{V} \setminus \{\mathcal{V}_k, \mathcal{E}_k, \mathcal{V}_{k+1}\}$,
- the case $k = d$ is identical to the case $k = 1$.

□

Lemma 2. *In the context of Lemma 1, for any $x \in \mathcal{V}$, for all $k \in \{1, \dots, d\}$ and $i \in \mathcal{E}_k$, the transition probabilities $\bar{P}^t(x, i)$ and $\bar{P}^{*t}(x, i)$ are conditionally independent of i given $i \in \mathcal{E}_k$.*

Proof. We prove Lemma 2 by recursion for $\bar{P}^t(x, i)$ only, the proof for $\bar{P}^{*t}(x, i)$ being identical. The initialisation follows from noting that for any i belonging to an edge connected to x , $\bar{P}(x, i) = 1/dn$. For any i belonging to an edge not connected to x , $\bar{P}(x, i) = 0$. As a consequence, for all i belonging to the same edge, $\bar{P}(x, i)$ is independent of i . Let us assume that for any $x \in \mathcal{V}$, for all $k \in \{1, \dots, d\}$, for all $i \in \mathcal{E}_k$, $\bar{P}^t(x, i) = \varrho_k^t(x)$, i.e. $\bar{P}^t(x, i)$ is independent of i . We have:

$$\begin{aligned} \bar{P}^{t+1}(x, i) &= \sum_{j \in \mathcal{X}} \bar{P}^t(x, j) \bar{P}(j, i), \\ &= \sum_{j \in \{\mathcal{V}_{k-1}, \mathcal{V}_k\}} \bar{P}^t(x, j) \bar{P}(j, i) + \sum_{j \in \mathcal{E}_k} \bar{P}^t(x, j) \bar{P}(j, i), \\ &= \sum_{j \in \{\mathcal{V}_{k-1}, \mathcal{V}_k\}} \bar{P}^t(x, j)/dn + \varrho_k^t(x) \sum_{j \in \mathcal{E}_k} \bar{P}(j, i), \end{aligned}$$

and since for all $(i, j) \in \mathcal{E}_k^2$, $\bar{P}(j, i)$ is independent of i , there exists $\rho_k^{t+1}(x)$ such that for all $i \in \mathcal{E}_k$, $\bar{P}^{t+1}(x, i) = \rho_k^{t+1}(x)$, which completes the proof. □

Lemma 3. *In the context of the proof of Proposition 2, $\gamma(\bar{P}) = \gamma(Q)$ and $\gamma(\bar{P}^*) = \gamma(Q^*)$.*

Proof. Without loss of generality and for notational simplicity, the proof is carried out in the case $\lambda = 1$, i.e. $\bar{P}_\lambda^* \equiv \bar{P}^*$. Central to this proof is the fact that $\Gamma\Omega = I_{2d+1}$, where Γ and Ω are the two change of basis matrices from \mathcal{Z} to its folded counterpart \mathcal{Y} and conversely, see their formal definition given at Algorithm 4. Indeed, it can be readily checked that Ω is an injection from \mathcal{Y} to \mathcal{Z} and thus admits a left inverse. This left inverse corresponds to the reverse transformation from \mathcal{Z} to \mathcal{Y} , which is precisely Γ .

We establish $\gamma(\bar{P}) = \gamma(Q)$ and $\gamma(\bar{P}^*) = \gamma(Q^*)$ is obtained in the same way.

Let $\lambda \in \text{Sp}(Q)$. Then, by definition of $\text{Sp}(P)$, there exists a non null vector $y_0 \in \mathbb{R}^{2d+1}$ such that

$$Qy_0 = \lambda y_0 \Leftrightarrow Q\Gamma\Omega y_0 = \lambda y_0 \Leftrightarrow \Omega Q\Gamma\Omega y_0 = \lambda \Omega y_0 \Leftrightarrow \bar{P}\Omega y_0 = \lambda \Omega y_0. \quad (51)$$

Moreover, since $\ker(\Omega)$ is restricted to the null vector 0_{2d+1} , $\Omega y_0 \neq 0_{(n-1)d+1}$ and $\lambda \in \text{Sp}(\bar{P})$.

Let $\lambda \in \text{Sp}(\bar{P})$, then, by definition of $\text{Sp}(\bar{P})$, there exists a non null vector $x_0 \in \mathbb{R}^{(n-1)d+1}$ such that, $\bar{P}x_0 = \lambda x_0$. By definition of \bar{P} , we have that

$$\Omega Q \Gamma x_0 = \lambda x_0 \Leftrightarrow \Gamma \Omega Q \Gamma x_0 = \lambda \Gamma x_0 \Leftrightarrow Q \Gamma x_0 = \lambda \Gamma x_0. \quad (52)$$

Now, $\ker(\Gamma)$ is not restricted to $0_{(n-1)d+1}$. Indeed, it can be readily checked that $x_0 := (0, 1, -1, 0, \dots, 0) \in \ker(\Gamma)$. As a consequence, for any $\lambda \in \text{Sp}(\bar{P})$ if the eigenvector associated λ does not belong to $\ker(\Gamma)$, then $\lambda \in \text{Sp}(Q)$. In contrast, if $x_0 \in \ker(\Gamma)$, it cannot be concluded whether or not $\lambda \in \text{Sp}(Q)$. A careful look at the transition matrix \bar{P} shows that the columns of \bar{P} are not linearly independent. In particular, the columns corresponding to states $x_0 \in Z$ belonging the same edge \mathcal{E}_k are all equal. As a consequence, $\text{rank}(\bar{P}) = 2d + 1$ which implies that $\dim(\ker(\bar{P})) = (n-1)d + 1 - 2d - 1 = (n-3)d$. This shows that $0 \in \text{Sp}(\bar{P})$ with multiplicity $(n-3)d$ and in fact $\ker(\Gamma) = \ker(\bar{P})$. Conversely, $\text{rank}(Q) = 2d + 1$ and thus $\dim(\ker(Q)) = 0$ which implies that $0 \notin \text{Sp}(Q)$. Combining those different observations yield to

$$\text{Sp}(\bar{P}) = \text{Sp}(Q) \cup 0. \quad (53)$$

The proof is concluded by noting that from the definition of the spectral gap, we have

$$\gamma(\bar{P}) = 1 - \sup_{\lambda \in \text{Sp}(\bar{P})} |\lambda| = 1 - \sup_{\lambda \in \text{Sp}(\bar{P}) \setminus \{0\}} |\lambda| = 1 - \sup_{\lambda \in \text{Sp}(Q)} |\lambda| = \gamma(Q). \quad (54)$$

□

Lemma 4. *In the context of Proposition 2 and whenever d is even, we have that*

$$\gamma(Q) = \gamma(Q_\lambda^*) \quad \text{for } \lambda = 2/d.$$

Proof of Lemma 4. The proof is established from the following series of steps

- calculating the characteristic polynomial for each matrix:

$$\chi(\lambda) = \det(Q - \lambda \text{Id}), \quad \chi_{2/d}^*(\lambda) = \det(Q_{2/d}^* - \lambda \text{Id})$$

- developing the determinant in a specific way, we show that χ and $\chi_{2/d}^*$ only differ through one factor:

$$\chi(\lambda) = \{n(d-1) - dn\lambda\}^2 \det M_\lambda, \quad \chi_{2/d}^*(\lambda) = \{n(d-2) + 1 - dn\lambda\}^2 \det M_\lambda.$$

- denoting $\Lambda = \{\lambda \in (-1, 1), \det M_\lambda = 0\}$, we have

$$\sigma(Q) = \left\{ 1, \quad \lambda_0 := \frac{d-1}{d}, \quad \Lambda \right\},$$

$$\sigma(Q_{2/d}^*) = \left\{ 1, \quad \lambda_0^* := \frac{d-2}{d} + \frac{1}{dn}, \quad \Lambda \right\}.$$

- for both cases, the larger eigenvalue smaller than 1 is in Λ . We first calculate the traces

$$\text{tr}(Q) = 2d - 1, \quad \text{tr}(Q_{2/d}^*) = 2d + \frac{2}{nd} - 1 - \frac{2}{d},$$

and since $\text{tr}(Q) = \sum_{\lambda \in \sigma(Q)} \lambda$, we have

$$\text{tr}(Q) = 1 + \lambda_0 + \sum_{\lambda \in \Lambda} \lambda, \quad \text{tr}(Q^*) = 1 + \lambda_0^* + \sum_{\lambda \in \Lambda} \lambda \quad (55)$$

If $\lambda_0 > \sup \Lambda$, then

$$1 + \lambda_0 + \sum_{\lambda \in \Lambda} \lambda < 1 + 2d\lambda_0 = 2d - 1 = \text{tr}(Q),$$

which contradicts the LHS of Eq. (55) and we have $\lambda_0 \leq \sup \Lambda$. Similarly, if $\lambda_0^* > \sup \Lambda$, then

$$1 + \lambda_0^* + \sum_{\lambda \in \Lambda} \lambda < 1 + 2d\lambda_0^* = 2d - 1 + 2\frac{1-n}{n} < \text{tr}(Q),$$

which contradicts the RHS of Eq. (55) and $\lambda_0^* \leq \sup \Lambda$. Therefore, regardless whether or not $(\lambda_0, \lambda_0^*) \in \Lambda^2$, the largest eigenvalue smaller than 1 of Q and $Q_{2/d}^*$ is identical. The proof is completed by showing that the spectral gaps of Q and $Q_{2/d}^*$ are identical.

□

Acknowledgements

Florian Maire would like to thank the Insight Centre for Data Analytics for funding the post-doc fellowship that allowed to develop this research. The Insight Centre for Data Analytics is supported by Science Foundation Ireland under Grant Number SFI/12/RC/2289.

References

- Andrieu, C. (2016). On random-and systematic-scan samplers. *Biometrika*, 103(3):719–726.
- Andrieu, C. and Thoms, J. (2008). A tutorial on adaptive MCMC. *Statistics and Computing*, 18(4):343–373.
- Bates, S. C., Cullen, A., and Raftery, A. E. (2003). Bayesian uncertainty assessment in multicompartiment deterministic simulation models for environmental risk assessment. *Environmetrics*, 14(4):355–371.
- Berezhkovskii, A. and Szabo, A. (2005). One-dimensional reaction coordinates for diffusive activated rate processes in many dimensions. *The Journal of chemical physics*, 122(1):014503.
- Beskos, A., Roberts, G. O., Thiery, A., and Pillai, N. (2018). Asymptotic analysis of the random-walk Metropolis algorithm on ridged densities. *The Annals of Applied Probability*, In Press.
- Buchete, N.-V. and Hummer, G. (2008). Coarse master equations for peptide folding dynamics. *The Journal of Physical Chemistry B*, 112(19):6057–6069.
- Carpenter, B., Gelman, A., Hoffman, M. D., Lee, D., Goodrich, B., Betancourt, M., Brubaker, M., Guo, J., Li, P., and Riddell, A. (2017). Stan: A probabilistic programming language. *Journal of Statistical Software*, 76(1).
- Chang, J. and Fisher, J. W. (2011). Efficient MCMC sampling with implicit shape representations. In *Computer Vision and Pattern Recognition (CVPR), 2011 IEEE Conference on*, pages 2081–2088. IEEE.

- Chauveau, D. and Vandekerkhove, P. (2013). Smoothness of Metropolis-Hastings algorithm and application to entropy estimation. ESAIM: Probability and Statistics, 17:419–431.
- Chauveau, D. and Vandekerkhove, P. (2014). Simulation based nearest neighbor entropy estimation for (adaptive) MCMC evaluation. In JSM Proceedings, Statistical Computing Section, pages 2816–2827. American Statistical Association, Alexandria, VA.
- Conrad, P. R., Marzouk, Y. M., Pillai, N. S., and Smith, A. (2016). Accelerating asymptotically exact MCMC for computationally intensive models via local approximations. Journal of the American Statistical Association, 111(516):1591–1607.
- Craiu, R. V., Rosenthal, J., and Yang, C. (2009). Learn from thy neighbor: Parallel-chain and regional adaptive MCMC. Journal of the American Statistical Association, 104(488):1454–1466.
- Diaconis, P., Holmes, S., and Shahshahani, M. (2013). Sampling from a manifold. In Advances in Modern Statistical Theory and Applications: A Festschrift in honor of Morris L. Eaton, pages 102–125. Institute of Mathematical Statistics.
- Douc, R., Moulines, E., and Rosenthal, J. S. (2004). Quantitative bounds on convergence of time-inhomogeneous Markov chains. Annals of Applied Probability, pages 1643–1665.
- Duan, Q., Sorooshian, S., and Gupta, V. (1992). Effective and efficient global optimization for conceptual rainfall-runoff models. Water Resources Research, 28(4):1015–1031.
- Duane, S., Kennedy, A. D., Pendleton, B. J., and Roweth, D. (1987). Hybrid Monte Carlo. Physics Letters B, 195(2):216–222.
- Erdil, E., Yildirim, S., Cetin, M., and Tasdizen, T. (2016). MCMC shape sampling for image segmentation with nonparametric shape priors. In Proceedings of the IEEE Conference on Computer Vision and Pattern Recognition, pages 411–419.
- Geman, S. and Geman, D. (1984). Stochastic relaxation, Gibbs distributions, and the Bayesian restoration of images. IEEE Transactions on Pattern Analysis and Machine Intelligence, (6):721–741.
- Girolami, M. and Calderhead, B. (2011). Riemann manifold Langevin and Hamiltonian Monte Carlo methods. Journal of the Royal Statistical Society: Series B (Statistical Methodology), 73(2):123–214.
- Givens, G. H. and Raftery, A. E. (1996). Local adaptive importance sampling for multivariate densities with strong nonlinear relationships. Journal of the American Statistical Association, 91(433):132–141.
- Grinstead, C. M. and Snell, J. L. (2012). Introduction to probability. American Mathematical Soc.
- Knapik, B. T., van der Vaart, A. W., and van Zanten, J. H. (2011). Bayesian inverse problems with Gaussian priors. The Annals of Statistics, 39(5):2626–2657.
- Latuszynski, K., Roberts, G. O., and Rosenthal, J. S. (2013). Adaptive Gibbs samplers and related MCMC methods. The Annals of Applied Probability.

- Lindvall, T. (2002). Lectures on the coupling method. Courier Corporation.
- Liu, J. S., Wong, W. H., and Kong, A. (1994). Covariance structure of the Gibbs sampler with applications to the comparisons of estimators and augmentation schemes. Biometrika, 81(1):27–40.
- Liu, J. S., Wong, W. H., and Kong, A. (1995). Covariance structure and convergence rate of the Gibbs sampler with various scans. Journal of the Royal Statistical Society: Series B (Statistical Methodology), pages 157–169.
- Livingstone, S. (2015). Geometric ergodicity of the random walk Metropolis with position-dependent proposal covariance. arXiv preprint arXiv:1507.05780.
- Livingstone, S. and Girolami, M. (2014). Information-geometric Markov chain Monte Carlo methods using diffusions. Entropy, 16(6):3074–3102.
- Maire, F., Douc, R., and Olsson, J. (2014). Comparison of asymptotic variances of inhomogeneous Markov chains with application to Markov chain Monte Carlo methods. The Annals of Statistics, 42(4):1483–1510.
- Mallik, A. and Jones, G. L. (2017). Directional Metropolis-Hastings. arXiv preprint arXiv:1710.09759.
- Metropolis, N., Rosenbluth, A. W., Rosenbluth, M. N., Teller, A. H., and Teller, E. (1953). Equation of state calculations by fast computing machines. The Journal of Chemical Physics, 21(6):1087–1092.
- Neal, R. M. et al. (2011). MCMC using Hamiltonian dynamics. Handbook of Markov Chain Monte Carlo, 2(11).
- Peskun, P. H. (1973). Optimum Monte-Carlo sampling using Markov Chains. Biometrika, 60(3):607–612.
- Poole, D. and Raftery, A. E. (2000). Inference for deterministic simulation models: the Bayesian melding approach. Journal of the American Statistical Association, 95(452):1244–1255.
- Raftery, A. E. and Bao, L. (2010). Estimating and projecting trends in HIV/AIDS generalized epidemics using incremental mixture importance sampling. Biometrics, 66(4):1162–1173.
- Raftery, A. E., Givens, G. H., and Zeh, J. E. (1995). Inference from a deterministic population dynamics model for bowhead whales. Journal of the American Statistical Association, 90(430):402–416.
- Roberts, G. and Rosenthal, J. (1997). Geometric ergodicity and hybrid Markov chains. Electronic Communications in Probability, 2:13–25.
- Roberts, G. O., Gelman, A., Gilks, W. R., et al. (1997). Weak convergence and optimal scaling of random walk Metropolis algorithms. The Annals of Applied Probability, 7(1):110–120.
- Roberts, G. O. and Rosenthal, J. S. (1998a). On convergence rates of Gibbs samplers for uniform distributions. The Annals of Applied Probability, 8(4):1291–1302.
- Roberts, G. O. and Rosenthal, J. S. (1998b). Two convergence properties of hybrid samplers. The Annals of Applied Probability, 8(2):397–407.

- Roberts, G. O. and Stramer, O. (2002). Langevin diffusions and Metropolis-Hastings algorithms. Methodology and Computing in Applied Probability, 4(4):337–357.
- Rosenthal, J. S. (1995). Minorization conditions and convergence rates for Markov chain Monte Carlo. Journal of the American Statistical Association, 90(430):558–566.
- Rosenthal, J. S. (2003). Asymptotic variance and convergence rates of nearly-periodic markov chain monte carlo algorithms. Journal of the American Statistical Association, 98(461):169–177.
- Tempel, E. and Bussov, M. (2014). Filamentary pattern in the cosmic web: galaxy filaments as pearl necklaces. Proceedings of the International Astronomical Union, 11(S308):236–241.
- Tierney, L. (1998). A note on Metropolis-Hastings kernels for general state spaces. The Annals of Applied Probability, pages 1–9.
- van de Weygaert, R., Jones, B. J., Platen, E., and Aragón-Calvo, M. A. (2009). Geometry and morphology of the cosmic web: Analyzing spatial patterns in the universe. In Voronoi Diagrams, 2009. ISVD'09. Sixth International Symposium on, pages 3–30. IEEE.